

Non-thermal radiation of cosmological γ -ray bursters

M.V. Smolsky and V.V. Usov

Department of Condensed-Matter Physics, Weizmann Institute of Science, Rehovot 76100,
Israel

ABSTRACT

We use one-and-a-half dimensional particle-in-cell plasma simulations to study the interaction of a relativistic, strongly magnetized wind with an ambient medium. Such an interaction is a plausible mechanism which leads to generation of cosmological γ -ray bursts. We confirm the idea of Mészáros and Rees (1992) that an essential part (about 20%) of the energy that is lost by the wind in the process of its deceleration may be transferred to high-energy electrons and then to high-frequency (X-ray and γ -ray) emission. We show that in the wind frame the spectrum of electrons which are accelerated at the wind front and move ahead of the front is nearly a two-dimensional relativistic Maxwellian with a relativistic temperature $T = m_e c^2 \Gamma_T / k \simeq 6 \times 10^9 \Gamma_T$ K, where Γ_T is equal to $200\Gamma_0$ with the accuracy of $\sim 20\%$, and Γ_0 is the Lorentz factor of the wind, $\Gamma_0 \gtrsim 10^2$ for winds outflowing from cosmological γ -ray bursters. Our simulations point to an existence of a high-energy tail of accelerated electrons with a Lorentz factor of more than $\sim 700\Gamma_0$. Large-amplitude electromagnetic waves are generated by the oscillating currents at the wind front. The mean field of these waves ahead of the wind front is an order of magnitude less than the magnetic field of the wind. High-energy electrons which are accelerated at the wind front and injected into the region ahead of the front generate synchro-Compton radiation in the fields of large-amplitude electromagnetic waves. This radiation closely resembles synchrotron radiation and can reproduce the non-thermal radiation of γ -ray bursts observed in the Ginga and BATSE ranges (from a few keV to a few MeV). Synchrotron photons which are generated in the vicinity of the wind front may be responsible for the radiation of γ -ray bursts in the EGRET energy range above a few ten MeV. The spectrum of γ -ray bursts in high-energy γ -rays may extend, in principle, up to the maximum energy of the accelerated electrons which is about $10^{13}(\Gamma_0/10^2)^2$ eV in the frame of the γ -ray burster.

Subject headings: acceleration of particles — radiation mechanism:
nonthermal — gamma-ray: bursts — gamma-rays: theory

1. Introduction

Many ideas about the nature of γ -ray bursts have been discussed during last 25 years after their discovery (for a review, see Blaes 1994; Harding 1994; Hartmann 1995; Dermer & Weiler 1995; Fishman & Meegan 1995; Greiner 1998; Piran 1998). Among these ideas, there was a suggestion that the sources of γ -ray bursts (GRBs) are at cosmological distances, i.e. at a redshift $z \sim 1$ (Usov & Chibisov 1975; van den Berg 1983; Paczyński 1986; Goodman 1986; Eichler et al. 1989). After the BATSE data became available (Meegan et al. 1992, 1994), the idea of a cosmological origin of GRB sources has come to be taken very seriously (e.g., Paczyński 1991; Fishman & Meegan 1995). Recent detections of absorption and emission features at a redshift $z = 0.835$ in the optical afterglow of GRB 970508 (Metzger et al. 1997) and at redshift $z = 3.42$ in the host galaxy of GRB 971214 (Kulkarni et al. 1998) clearly demonstrate that at least some of the GRB sources lie at cosmological distances. A common feature of all acceptable models of cosmological γ -ray bursters is that a relativistic wind is a source of GRB radiation. The Lorentz factor, Γ_0 , of such a wind is about $10^2 - 10^3$ or even more (e.g., Fenimore, Epstein, & Ho 1993; Baring and Harding 1997). A very strong magnetic field may be in the plasma outflowing from cosmological γ -ray bursters (Usov 1992, 1994a,b; Thompson & Duncan 1993; Blackman, Yi, & Field 1996; Vietri 1996; Katz 1997; Mészáros & Rees 1997a; Dai & Lu 1998). It was pointed out (Mészáros & Rees 1992, 1993; Rees & Mészáros 1992) that the kinetic energy of relativistic winds may be converted into non-thermal radiation of GRBs when these winds interact with an ambient medium (e.g., an ordinary interstellar medium or plasma which is ejected from the predecessor of the burster). Recently, the interaction between a relativistic magnetized wind and an ambient medium was studied numerically (Smolsky & Usov 1996; Usov & Smolsky 1998), and it was shown that electrons of the ambient medium which are reflected from the wind front are accelerated up to the mean energy of reflected protons. In this paper we study both the spectrum of electrons accelerated at the wind front and their non-thermal radiation.

A plausible model of cosmological GRBs is discussed in § 2. The main results of our numerical simulations of the interaction between a relativistic strongly magnetized wind and an ambient medium are presented in § 3. The spectrum of electrons which are accelerated at the wind front and their non-thermal radiation are considered in § 4. Finally, our main conclusions are summarized and discussed in § 5.

2. Relativistic strongly magnetized winds from cosmological γ -ray bursters and their non-thermal radiation: a plausible scenario

The energy output of cosmological γ -ray bursters in γ -rays typically is $10^{51} - 10^{53}$ ergs (Wikramasinghe et al. 1993; Tamblyn & Melia 1993; Lipunov et al. 1995) and may be as high as 3×10^{53} ergs (Kulkarni et al. 1998) or even more (Kulkarni et al. 1999). These estimates assume isotropic emission of GRBs. Such a high energetics of cosmological γ -ray bursters and a short time scale of γ -ray flux variability call for very compact objects as sources of GRBs (Hartmann 1995; Piran 1998 and references therein). These objects may be either millisecond pulsars which are arisen from accretion-induced collapse of white dwarfs in close binaries (Usov 1992) or differentially rotating disk-like objects which are formed by the merger of a binary consisting of two neutron stars (Eichler et al. 1989; Narayan, Paczyński, & Piran 1992). Such very young fast-rotating compact objects have two possible sources of energy which may be responsible for radiation of cosmological GRBs. These are the thermal energy of the compact objects and the kinetic energy of their rotation. The thermal energy may be transformed into γ -rays by means of the following sequence of processes (for review, see Piran 1998): (1) Emission of neutrinos and cooling of the object; (2) Absorption of neutrinos ($\nu_i + \bar{\nu}_i \rightarrow e^+ + e^-$) and formation of a fireball which mainly consists of electrons and positrons; (3) Expansion of the fireball and formation of a relativistic shell, $\Gamma_0 \gtrsim 10^2$; (4) Interaction of the shell with an external medium and acceleration of electrons to very high energies; and (5) Generation of γ -rays by high-energy electrons. The maximum thermal energy, $Q_{\text{th}}^{\text{max}}$, of very young compact objects is high enough to explain the energy output of cosmological GBBs, $Q_{\text{th}}^{\text{max}} \simeq \text{a few} \times 10^{53}$ ergs. However, the fraction of the thermal energy that is converted into the energy of the electron-positron fireball and then into the kinetic energy of the relativistic shell is very small and cannot be essentially more than $10^{-3} - 10^{-2}$ (Goodman, Dar & Nussinov 1987; Eichler et al. 1989; Janka & Ruffert 1996; Piran 1998 and references therein). Moreover, the efficiency of transformation of the kinetic energy of a relativistic shell into radiation cannot be more than 30 – 40% (Blandford & Eichler 1987). Hence, neutrino powered winds outflowing from compact objects may be responsible for the radiation of cosmological GRBs only if they are well collimated, with opening angle about a few degrees or even less. For both young neutron stars and post-merger objects, such a collimation of neutrino powered winds is very questionable (e.g., Woosley 1993; Piran 1998 and references therein).

The rotational energy of the compact objects at the moment of their formation may be comparable with the thermal energy, $Q_{\text{rot}}^{\text{max}} \simeq Q_{\text{th}}^{\text{max}}$. The efficiency of transformation of the rotational energy to the energy of a relativistic strongly magnetized wind and then to the energy of high-frequency radiation may be as high as almost 100% (see Usov 1994a,b; Blackman et al. 1996 and below). For some time the theoretical expectation has been that

rotation powered neutron stars (pulsars) should generate collimated outflows (e.g., Benford 1984; Michel 1985; Sulkanen & Lovelace 1990). The Crab, Vela, PSR B1509-58 and possible PSR B1951+32 all show evidence that this is indeed the case (Hester 1998; Gaensler et al. 1999 and references therein). If the energy flux from the source of GRB 990123 in the direction to the Earth is only about ten times more than the energy flux averaged over all directions, the model of GRBs based on the rotation powered winds can easily explain the energetics of such an extremal event as GRB 990123 (Kulkarni et al. 1999). Such an anisotropy of emission from the burst sources doesn't contradict available data on GRBs (e.g., Perna & Loeb 1998). In the case of typical GRBs with the energy output of $10^{51} - 10^{53}$ ergs, this model can explain their energetics even if the emission of GRBs is nearly isotropic. Therefore, the rotational energy of compact objects is a plausible source of energy for cosmological GRBs, not the thermal energy.

In many papers (e.g., Usov 1992; Thompson & Duncan 1993; Blackman et al. 1996; Kluźniak & Ruderman 1998), it was argued that the strength of the magnetic field B_s at the surface of compact objects may be as high as $\sim 10^{16}$ G or even more. Such a strong magnetic field leads to both deceleration of the rotation of the fast-rotating compact object on a time scale of seconds and generation of a strongly magnetized wind that flows away from the object at a relativistic speed, $\Gamma_0 \simeq 10^2 - 10^3$ (e.g., Usov 1994a). The outflowing wind is Poynting flux-dominated, i.e., $\sigma = L_{\pm}/L_p \ll 1$, where

$$L_p \simeq \frac{2 B_s^2 R^6 \Omega^4}{3 c^3} \simeq 2 \times 10^{52} \left(\frac{B_s}{10^{16} \text{ G}} \right)^2 \left(\frac{R}{10^6 \text{ cm}} \right)^6 \left(\frac{\Omega}{10^4 \text{ s}^{-1}} \right)^4 \text{ ergs s}^{-1} \quad (1)$$

is the luminosity of the compact object in the Poynting flux, L_{\pm} is its luminosity in both electron-positron pairs and radiation, c is the speed of light, R is the radius of the compact object and Ω is its angular velocity; $R \sim 10^6$ cm and $\Omega \sim 10^4$ s $^{-1}$ for both millisecond pulsars and post-merger objects. For compact objects with extremely strong magnetic fields, $B_s \sim 10^{16}$ G, it is expected that σ is $\sim 0.01 - 0.1$ (Usov 1994a).

A plausible magnetic topology for a relativistic magnetized wind outflowing from an oblique rotator ($\vartheta \neq 0$) with a nearly dipole magnetic field is shown in Figure 1, where ϑ is the angle between the rotational axis and the magnetic axis. Near the rotational poles, the wind field should be helical (e.g., Coroniti 1990). This is because the magnetic flux originates in a single polar cap. Near the rotational equator, the toroidal magnetic field of the wind should be striped and alternates in polarity on a scalelength of $\pi(c/\Omega) \sim 10^7$ cm. These magnetic stripes are separated by thin current sheets (J_{θ}). Off the equator, the magnetic flux in the toward and away stripes is unequal if $\vartheta \neq \pi/2$. In other words, in the striped region, the wind field is a superposition of a pure helical field and a pure striped

field with nearly equal magnetic fluxes in adjacent stripes.

Since the luminosity of a γ -ray burster in a relativistic magnetized wind drops in time, $L_p \propto t^{-\beta}$, the wind structure at the moment $t \gg \tau_\Omega$ is similar to a shell with the radius $r \simeq ct$, where β is a numerical index, $1 \leq \beta \leq 2$, and $\tau_\Omega \sim 10^{-2} - 10^2$ s is the characteristic time of deceleration of the compact object rotation due to the action of the electromagnetic torque and the torque related to generation of gravitational radiation (Usov 1992; Yi & Blackman 1998). The thickness of the shell is $\sim c\tau_\Omega$.

The strength of the magnetic field at the front of the wind is about

$$B \simeq B_s \frac{R^3}{r_{lc}^2 r} \simeq 10^{15} \frac{R}{r} \left(\frac{B_s}{10^{16} \text{ G}} \right) \left(\frac{\Omega}{10^4 \text{ s}^{-1}} \right)^2 \text{ G}, \quad (2)$$

where $r_{lc} = c/\Omega = 3 \times 10^6 (\Omega/10^4 \text{ s}^{-1})$ cm is the radius of the light cylinder.

Non-thermal radiation from a relativistic strongly magnetized wind depends on whether the wind is striped in the direction of its outflow or not. If the wind is striped (see Fig.1), the magnetic field is more or less frozen in the outflowing plasma at the distance $r \lesssim r_f$ (Usov 1994a; Blackman & Yi 1998), where

$$r_f \simeq 2 \times 10^{14} \sigma^{3/4} \left(\frac{B_s}{10^{16} \text{ G}} \right)^{1/2} \left(\frac{\Omega}{10^4 \text{ s}^{-1}} \right)^{1/2} \text{ cm}. \quad (3)$$

At $r > r_f$, the wind density is not sufficient to screen displacement currents, and the striped component of the wind field is transformed into large-amplitude electromagnetic waves (LAEMWs) due to development of magneto-parametric instability (Usov 1975, 1994a,b; Blackman et al. 1996; Melatos & Melrose 1996a,b). [For a criterion for electromagnetic waves to be considered as LAEMWs see § 4.] The typical frequency of generated LAEMWs is equal to Ω , and their amplitude is $\sim B$. Outflowing particles are accelerated in the field of LAEMWs to Lorentz factors of the order of 10^6 , and generate non-thermal synchro-Compton radiation with the typical energy of photons in the range of a few $\times (0.1 - 1)$ MeV (Usov 1994a,b; Blackman et al. 1996; Blackman & Yi 1998). A long high-energy tail of the γ -ray spectrum may exist up to $\sim 10^4$ MeV. This is consistent with the observed spectra of GRBs (Band et al. 1993; Schaefer et al. 1994; Fishman & Meegan 1995).

The radiative damping length for LAEMWs generated at $r \sim r_f$ is a few orders of magnitude less than r_f (Usov 1994a). Therefore, at $r \gg r_f$ LAEMWs decay almost completely, and their energy is transferred to high-energy electrons and then to X-ray and

γ -ray photons. It is worth noting that when the magnetic axis is perpendicular to the rotational axis, $\vartheta = \pi/2$, the electromagnetic field of the Poynting flux-dominated wind is purely striped just as vacuum magnetic dipole waves (Michel 1971). In this case, almost all energy of the wind is radiated in X-rays and γ -rays at $r \sim r_f$ (Usov 1994a; Blackman, Yi, & Field 1996; Blackman & Yi 1998), and the total energy output in hard photons per a GRB may be as high as $Q_{\text{rot}}^{\text{max}} \simeq \text{a few} \times 10^{53}$ ergs.

At $r \gg r_f$ and $\vartheta \neq \pi/2$, the magnetic field is helical everywhere in the outflowing wind (see Fig. 1). Such a relativistic strongly magnetized wind expands more or less freely up to the distance

$$r_{\text{dec}} \simeq 5 \times 10^{16} \left(\frac{Q_{\text{kin}}}{10^{52} \text{ ergs}} \right)^{1/3} \left(\frac{n}{1 \text{ cm}^{-3}} \right)^{-1/3} \left(\frac{\Gamma_0}{10^2} \right)^{-2/3} \text{ cm}, \quad (4)$$

at which deceleration of the wind due to its interaction with an ambient medium becomes important (Rees & Mészáros 1992), where n is the density of the ambient medium and Q_{kin} is the kinetic energy of the outflowing wind, $Q_{\text{kin}} \leq Q_{\text{rot}} \leq Q_{\text{rot}}^{\text{max}}$. Substituting r_{dec} for r into equation (2), we have the following estimate for the magnetic field at the wind front at $r \sim r_{\text{dec}}$:

$$B_{\text{dec}} \simeq 2 \times 10^4 \left(\frac{B_s}{10^{16} \text{ G}} \right) \left(\frac{\Omega}{10^4 \text{ s}^{-1}} \right)^2 \left(\frac{Q_{\text{kin}}}{10^{52} \text{ ergs}} \right)^{-1/3} \left(\frac{n}{1 \text{ cm}^{-3}} \right)^{1/3} \left(\frac{\Gamma_0}{10^2} \right)^{2/3} \text{ G}, \quad (5)$$

For typical parameters of cosmological γ -ray bursters, $B_s \simeq 10^{16}$ G, $\Omega \simeq 10^4 \text{ s}^{-1}$, $Q_{\text{kin}} \simeq 10^{52} - 10^{53}$ ergs and $\Gamma_0 \simeq 10^2 - 10^3$, if the ambient medium is an ordinary interstellar gas, $n \sim 1 - 10^2 \text{ cm}^{-3}$, from equation (5) we have $B_{\text{dec}} \simeq 10^4 - 4 \times 10^5$ G.

It is suggested by Mészáros and Rees (1992) that in the process of the wind – ambient medium interaction at $r \sim r_{\text{dec}}$, an essential part of the wind energy may be transferred to high-energy electrons and then to high-frequency (X-ray and γ -ray) emission. This suggestion is confirmed by our numerical simulations (see Smolsky & Usov 1996; Usov & Smolsky 1998 and below). Hence, in our scenario in a general case, when the rotational axis and the magnetic axis are not aligned ($\vartheta \neq 0$) or perpendicular ($\vartheta \neq \pi/2$), there are at least two regions where powerful non-thermal X-ray and γ -ray emission of GRBs may be generated. The first region is at $r \sim r_f \sim 10^{13} - 10^{14}$ cm, and the second one is at $r \sim r_{\text{dec}} \sim 10^{16} - 10^{17}$ cm. Acceleration of electrons and their radiation in the first radiating region at $r \sim r_f$ were considered in details earlier (Usov 1994a,b; Blackman et al. 1996; Blackman & Yi 1998). Below, we consider the spectrum of electrons accelerated at $r \sim r_{\text{dec}}$ and their radiation.

3. Interaction of a relativistic strongly magnetized wind with an ambient medium

For consideration of the interaction between a relativistic magnetized wind and an ambient medium, it is convenient to switch to the co-moving frame of the outflowing plasma (the wind frame). While changing the frame, the magnetic and electric fields in the wind are reduced from B and $E = B[1 - (1/\Gamma_0^2)]^{1/2} \simeq B$ in the frame of the γ -ray burster to $B_0 \simeq B/\Gamma_0$ and $E_0 = 0$ in the wind frame. Using this and equation (5), for typical parameters of cosmological γ -ray bursters (see § 2) we have $B_0 \simeq 10^2 - 10^3$ G at $r \simeq r_{\text{dec}}$.

In the wind frame, the problem of the wind – ambient medium interaction is identical to the problem of collision between a wide relativistic beam of cold plasma and a region with a strong magnetic field which is called a magnetic barrier. Recently, the interaction of a wide relativistic plasma beam with a magnetic barrier was studied numerically (Smolsky & Usov 1996; Usov & Smolsky 1998). In these studies, the following initial condition of the beam – barrier system was assumed. Initially, at $t = 0$, the ultrarelativistic homogeneous neutral beam of protons and electrons (number densities $n_p = n_e \equiv n_0$) runs along the x axis and impacts at the barrier, where n_0 is constant. The beam is infinite in the $y - z$ dimensions and semi-infinite in the x dimension. The magnetic field of the barrier \mathbf{B}_0 is uniform and transverse to the beam velocity, $\mathbf{B}_0 = B_0 \hat{\mathbf{e}}_z \Theta[x]$, where B_0 is constant and $\Theta[x]$ is the step function equal to unity for $x > 0$ and to zero for $x < 0$. At the front of the barrier, $x = 0$, the surface current J_y runs along the y axis to generate the jump of the magnetic field. The value of this current per unit length of the front across the current direction is $cB_0/4\pi$. A $1\frac{1}{2}$ D time-dependent solution for the problem of the beam – barrier interaction was constructed, i.e., electromagnetic fields ($\mathbf{E} = E_x \hat{\mathbf{e}}_x + E_y \hat{\mathbf{e}}_y$; $\mathbf{B} = B \hat{\mathbf{e}}_z$) and motion of the beam particles in the $x - y$ plane were found. The structure of the fields and motion of the beam particles were treated self-consistently except the external current J_y which was fixed in our simulations.

The main results of our simulations are the following (Smolsky & Usov 1996; Usov & Smolsky 1998).

1. When the energy densities of the beam and the magnetic field, \mathbf{B}_0 , of the barrier are comparable,

$$\alpha = 8\pi n_0 m_p c^2 (\Gamma_0 - 1) / B_0^2 \sim 1, \quad (6)$$

where m_p is the proton mass, the process of the beam – barrier interaction is strongly nonstationary, and the density of protons after their reflection from the barrier is strongly

non-uniform. The ratio of the maximum density of reflected protons and their minimum density is ~ 10 .

2. At $\alpha > \alpha_{\text{cr}} \simeq 0.4$, the depth of the beam particle penetration into the barrier increases in time, $x_{\text{pen}} \simeq v_{\text{pen}}t$, where v_{pen} is the mean velocity of the penetration into the barrier. The value of v_{pen} is subrelativistic and varies from zero (no penetration) at $\alpha \leq \alpha_{\text{cr}}$ to $0.17c$ at $\alpha = 1$ and then to $0.32c$ at $\alpha = 2$. At $\alpha > \alpha_{\text{cr}}$, the magnetic field of the barrier at the moment t roughly is $B(t) \simeq B_0\Theta[x - x_{\text{pen}}(t)]$ (see Fig. 2). In other words, the front of the beam – barrier interaction is displaced into the barrier with the velocity v_{pen} . For $\alpha > \alpha_{\text{cr}}$, our consideration of the beam – barrier interaction in the vicinity of the new front, $x \simeq x_{\text{pen}}$, is *completely self-consistent*, and no simplifying assumptions besides geometrical ones are exploited.

3. At the front of the barrier, $x \simeq x_{\text{pen}}(t)$, the surface current varies in time because of strong nonstationarity of the beam – barrier interaction at $\alpha \sim 1$, and low-frequency electromagnetic waves are generated (Fig. 2). The typical frequency of these waves is about the proton gyrofrequency $\omega_{Bp} = eB_0/m_p c\Gamma_0$ in the field of the barrier B_0 . The wave amplitude B_w can reach $\sim 0.2B_0$.

4. At $\alpha \sim 1$, strong electric fields are generated in the vicinity of the front of the barrier, $x \simeq x_{\text{pen}}(t)$, and electrons of the beam are accelerated in these fields up to the mean energy of protons, i.e. up to $\sim m_p c^2 \Gamma_0$ (see Fig. 3). At $\alpha_{\text{cr}} < \alpha \lesssim 1$, the mean Lorentz factor of outflowing high-energy electrons after their reflection and acceleration at the barrier front depends on α and is

$$\langle \Gamma_e^{\text{out}} \rangle \simeq 0.2 \left(\frac{m_p}{m_e} \right) \Gamma_0 \quad (7)$$

within a factor of 2. The total energy of accelerated electrons is about 20% of the energy in outflowing protons which are reflected from the magnetic barrier.

5. At $\alpha_{\text{cr}} < \alpha \lesssim 1$, the mean Lorentz factor of protons reflected from the barrier is $\langle \Gamma_p^{\text{out}} \rangle \simeq (0.7 \pm 0.1)\Gamma_0$, i.e. the process of the beam proton reflection from the barrier is non-elastic, and about 30% of the initial kinetic energy of the beam protons is lost in this collision. The energy that is lost by the beam protons is transferred to high-energy electrons and low-frequency electromagnetic waves. Typically, the energy in these waves is a few times smaller than the energy in high-energy electrons.

In the burster frame, a magnetized wind flows away from the burster at relativistic speeds and collides with an ambient medium. In the process of such a collision, the outflowing wind loses its energy. From the listed results of our simulations of the beam –

barrier collision (Smolsky & Usov 1996; Usov & Smolsky 1998), it follows that at $r \sim r_{\text{dec}}$, where α is ~ 1 , about 70% of the energy losses of the wind are transferred to protons of the ambient medium which are reflected from the wind front. The mean energy of reflected protons is about $m_p c^2 \Gamma_0^2$. The other 30% of the wind energy losses are distributed between high-energy electrons and low-frequency electromagnetic waves. As a rule, the total energy in accelerated electrons is a few times more than the total energy in low-frequency waves.

4. Non-thermal radiation from the region of the wind – ambient medium interaction

High-energy electrons accelerated at the wind front generate non-thermal radiation while they move in both the magnetic field of the wind and the electromagnetic fields of low-frequency waves that are produced by the non-stationary currents at the wind front.

4.1. Synchrotron radiation from the wind front

In our simulations of the beam – magnetic barrier interaction (Smolsky & Usov 1996; Usov & Smolsky 1998), the examined space-time domain is

$$x_{\min} < x < x_{\max}, \quad 0 < t < t_{\max}, \quad (8)$$

where x_{\max} and $-x_{\min}$ are equal to a few $\times (1-10)(c/\omega_{Bp})$, t_{\max} is equal to a few $\times (1-10)T_p$, and (c/ω_{Bp}) and $T_p = 2\pi/\omega_{Bp}$ are the proton gyroradius and gyroperiod in the magnetic field of the barrier B_0 , respectively. Non-thermal radiation of high-energy electrons from the examined space domain was calculated for the beam and barrier parameters which are relevant to cosmological GRBs (Smolsky & Usov 1996; Usov & Smolsky 1998). Figure 4 shows the intensity of radiation as a function of time t for a simulation with $B_0 = 300$ G, $\Gamma_0 = 300$, $\alpha = 2/3$, $x_{\min} = -5(c/\omega_{Bp})$ and $x_{\max} = 30(c/\omega_{Bp})$. In all our simulations, the bulk of calculated radiation is generated via synchrotron mechanism in a compact vicinity, $x_{\text{pen}} - 2(c/\omega_{Bp}) < x < x_{\text{pen}}$, of the barrier front where both the strength of the magnetic field is of the order of B_0 and the mean energy of accelerated electrons is extremely high. Radiation of high-energy electrons in the fields of low-frequency waves is negligible ($\sim 1\%$ or less) because both the fields of these waves are about an order of magnitude smaller than B_0 (see below) and the length of the examined space domain (8) is restricted for computational reasons.

At $\alpha \sim 1$, the mean energy of synchrotron photons generated at the front of the barrier is

$$\langle \varepsilon_\gamma \rangle \simeq 0.1 \left(\frac{\Gamma_0}{10^2} \right)^2 \left(\frac{B_0}{10^3 \text{ G}} \right) \text{ MeV}. \quad (9)$$

The average fraction of the kinetic energy of the beam that is radiated in these photons is

$$\xi_\gamma \equiv \frac{\langle \Phi_\gamma \rangle}{n_0 m_p c^3 \Gamma_0} \simeq 10^{-3} \left(\frac{\Gamma_0}{10^2} \right)^2 \left(\frac{B_0}{10^3 \text{ G}} \right), \quad (10)$$

where $\langle \Phi_\gamma \rangle$ is the average synchrotron luminosity of high-energy electrons per unit area of the barrier front.

In the burster frame, the characteristic energy, $\langle \tilde{\varepsilon}_\gamma \rangle$, of synchrotron photons generated in the vicinity of the wind front increases due to the Doppler effect. Taking this into account and using equation (9), we have

$$\langle \tilde{\varepsilon}_\gamma \rangle \simeq 10 \left(\frac{\Gamma_0}{10^2} \right)^2 \left(\frac{B_{\text{dec}}}{10^5 \text{ G}} \right) \text{ MeV}. \quad (11)$$

where B_{dec} is determined in equation (5). The fraction of the wind energy which is transferred to radiation at the wind front does not depend on the frame where it is estimated, and in the burster frame it is equal to

$$\tilde{\xi}_\gamma = \xi_\gamma \simeq 10^{-3} \left(\frac{\Gamma_0}{10^2} \right) \left(\frac{B_{\text{dec}}}{10^5 \text{ G}} \right), \quad (12)$$

For typical parameters of relativistic magnetized winds which are relevant to cosmological γ -ray bursters, $\Gamma_0 \simeq 10^2 - 10^3$ and $B_{\text{dec}} \simeq 10^5 \text{ G}$ (see § 2), from equations (11) and (12) we have $\langle \tilde{\varepsilon}_\gamma \rangle \simeq 10 - 10^3 \text{ MeV}$ and $\tilde{\xi} \simeq 10^{-2} - 10^{-3}$, i.e., the synchrotron radiation that is generated at wind front is in the EGRET range.

The main part of X-ray and γ -ray emission of detected GRBs is in the BATSE range, from a few $\times 10 \text{ keV}$ to a few MeV (e.g., Fishman & Meegan 1995). Synchrotron radiation from the wind front is either too hard or too weak to explain this emission irrespective of B_{dec} . Indeed, equations (11) and (12) yield

$$\langle \tilde{\varepsilon}_\gamma \rangle \simeq 10^2 \left(\frac{\Gamma_0}{10^2} \right) \left(\frac{\tilde{\xi}_\gamma}{10^{-2}} \right) \text{ MeV}. \quad (13)$$

In our model, the energy of rotation powered winds which are responsible for cosmological GRBs cannot be significantly more than 10^{53} ergs. To explain the energy output of $\sim 10^{51} - 10^{53}$ ergs per GRB (see § 2), the efficiency of transformation of the wind energy into the energy of non-thermal radiation has to be about or more than 1%, $\tilde{\xi}_\gamma \gtrsim 10^{-2}$, and for some GRBs it may be as high as 100%, $\tilde{\xi}_\gamma \simeq 1$. Taking into account that for cosmological GRBs the value of Γ_0 is $\gtrsim 10^2$ (e.g., Fenimore, Epstein, & Ho 1993; Baring and Harding 1997), for $\tilde{\xi}_\gamma \gtrsim 10^{-2}$ from equation (13) it follows that the mean energy of synchrotron photons generated at the wind front is very high, $\langle \tilde{\varepsilon}_\gamma \rangle \gtrsim 100$ MeV. This is because the bulk of these photons is generated in the thin vicinity of the wind front where there are both a strong magnetic field, $B \simeq B_0$, and high-energy electrons. The mean time that high-energy electrons spend in this vicinity and generate synchrotron radiation is very short, \sim a few $\times T_p \sim 10^{-6} (B_{\text{dec}}/10^5 \text{ G})^{-1} (\Gamma_0/10^2)$ s. To get a high efficiency of synchrotron radiation at the wind front, $\tilde{\xi}_\gamma > 10^{-2}$, it is necessary to assume that the magnetic field B_{dec} is about its maximum value (see § 2). From equation (11), we can see that in this case the mean energy of synchrotron photons is of the order of or higher than 10^2 MeV.

For a typical value of B_{dec} , that is $\sim 10^5$ G (see § 2), and $\Gamma_0 \sim 10^2 - 10^3$, from equation (12) we have $\tilde{\xi}_\gamma \sim 10^{-3} - 10^{-2} \ll 1$. Hence, high-energy electrons are accelerated at the wind front and injected into the region ahead of the front practically without energy losses. In our model, these high-energy electrons are the best candidates to be responsible for the X-ray and γ -ray emission of GRBs in the BATSE range. Before considering high-frequency radiation from the region ahead of the wind front, we discuss briefly some general properties of radiation of high-energy electrons in the fields of electromagnetic waves.

4.2. LAEMWs and synchro-Compton radiation of electrons

The motion of electrons and their radiation in the fields of electromagnetic waves is characterized by the following dimensionless Lorentz-invariant parameter (e.g., Blumenthal & Tucker 1974):

$$\eta = \frac{eB_w}{m_e c \omega}, \quad (14)$$

where B_w is the amplitude of the waves and ω is their frequency. At $\eta \ll 1$, electrons radiate via Compton scattering. In this case, the typical energy of photons $\langle \varepsilon_c \rangle$ after scattering depends on the wave frequency, $\langle \varepsilon_c \rangle \propto \omega \Gamma_e^2$, and does not depend on the wave amplitude (e.g., Blumenthal & Tucker 1974).

Electromagnetic waves with $\eta \gg 1$ are called large-amplitude electromagnetic waves (LAEMWs). Radiation of electrons in the fields of LAEMWs is called synchro-Compton radiation. In the most simple case which is interesting for us (see below) when the bulk of radiating electrons has such a high velocity $v_{\perp} = c \sin \psi$ transverse to the wave vector that

$$(v_{\perp}/c)\Gamma_e = \Gamma_e \sin \psi \gtrsim \eta, \quad (15)$$

synchro-Compton radiation of these electrons closely resembles synchrotron radiation (Blumenthal & Tucker 1974), where ψ is the angle between the electron velocity and the wave vector of LAEMWs. Indeed, it is well known that electromagnetic radiation of relativistic electrons is concentrated in the direction of the particle's velocity within a narrow cone of angle $\Delta\varphi \simeq 1/\Gamma_e \ll 1$ (e.g., Rybicki & Lightman 1979). For nearly transverse motion of electrons in a magnetic field B , the formation length of radiation is about $\Delta l \simeq 2R_{Be}\Delta\varphi \simeq 2m_e c^2/eB$, where $R_{Be} = m_e c^2 \Gamma_e / eB$ is the electron gyroradius. For synchro-Compton radiation, $\eta \gg 1$, the formation length is much smaller than the wavelength, $\lambda = 2\pi c/\omega$, of LAEMWs :

$$\Delta l \simeq \left(\frac{m_e c \omega}{\pi e B} \right) \lambda \simeq \frac{\lambda}{\pi \eta} \ll \lambda, \quad (16)$$

and the electromagnetic fields of LAEMWs may be considered as homogeneous and static. Therefore, synchro-Compton radiation is similar to synchrotron radiation in a magnetic field which is equal to the local field of LAEMWs. [For details on synchro-Compton radiation see (Gunn & Ostriker 1971; Blumenthal & Tucker 1974).]

The mean frequency of synchro-Compton radiation of high-energy electrons with the Lorentz factor Γ_e is (e.g., Blumenthal & Tucker 1974)

$$\nu_{sc} \simeq \frac{e \langle B_w \rangle \Gamma_e^2}{2\pi m c} \simeq 3 \times 10^6 \langle B_w \rangle \Gamma_e^2 \text{ Hz}, \quad (17)$$

where $\langle B_w \rangle$ is the mean field of LAEMWs.

4.3. LAEMWs generated at the wind front

At $\alpha \sim 1$, low-frequency electromagnetic waves are generated at the wind front and propagate in both directions from the front (see § 3 and Figs 2 and 5 – 7). These waves are non-monochromatic. Figure 8 shows a typical spectrum of low-frequency waves in the wind

frame. This spectrum has a maximum at the frequency ω_{\max} which is a few times higher than the proton gyrofrequency $\omega_{Bp} = eB_0/m_p c\Gamma_0$ in the field of B_0 .

At high frequencies, $\omega > \omega_{\max}$, the spectrum of low-frequency waves may be fitted by a power law:

$$|B(\omega)|^2 \propto \omega^{-\beta}, \quad (18)$$

where $\beta \simeq 1.6$.

In the region ahead of the wind front, the mean field of low-frequency waves depends on α , and in the wind frame, for $\alpha_{\text{cr}} \lesssim \alpha \lesssim 1$ this field is

$$\langle B_w \rangle = (\langle B_z \rangle^2 + \langle E_y \rangle^2)^{1/2} \simeq 0.1B_0 \simeq 0.1B_{\text{dec}}/\Gamma_0 \quad (19)$$

within a factor of 2 or so.

At $\alpha > 1$, the intensity of low-frequency waves is suppressed in the region ahead of the wind front (see Fig. 6) because the typical frequency, $\omega \simeq \omega_{\max}$, of these waves is smaller than the relativistic plasma frequency of the ambient medium, $\omega_p = (4\pi n_0 e^2/m_e \langle \Gamma_e \rangle)^{1/2}$ (Gallant et al. 1992). In this case, only a high-frequency component of low-frequency waves with the frequency $\omega \gtrsim \omega_p \simeq (5\alpha)^{1/2} \omega_{Bp}$ propagates far ahead of the wind front.

For typical parameters of low-frequency waves generated at the wind front, $B_w \simeq 0.1B_0$ and $\omega \simeq \omega_{\max} \simeq 3\omega_{Bp} \simeq 3(eB_0/m_p c\Gamma_0)$, from equation (14) we have

$$\eta \simeq \frac{B_w}{B_0} \frac{m_p}{m_e} \Gamma_0 \simeq 50\Gamma_0 \gg 1. \quad (20)$$

Hence, these low-frequency waves are LAEMWs.

4.4. High-energy electrons accelerated at the wind front

At $r \sim r_{\text{dec}}$, where α is ~ 1 , about 20% of the energy of a relativistic strongly magnetized wind is transferred to electrons of an ambient medium which are reflected from the wind front and accelerated to extremely high energies (see § 3 and references therein). In the wind frame, the spectrum of high-energy electrons in the region ahead of the wind front may be fitted by a two-dimensional relativistic Maxwellian

$$\frac{dn_e}{d\Gamma_e} \propto \Gamma_e \exp\left(-\frac{m_e c^2 \Gamma_e}{kT}\right) \quad (21)$$

with a relativistic temperature $T = m_e c^2 \Gamma_T / k$, where $\Gamma_T \simeq 240\Gamma_0$ (see Fig. 9). The fact that the energy distribution of accelerated electrons at $\alpha \sim 1$ is close to a relativistic Maxwellian is quite natural because at $\alpha \gtrsim \alpha_{\text{cr}}$ the trajectories of particles in the front vicinity are fully chaotic. The thermal distribution of high energy electrons does not come as a result of interparticle collisions, since the ambient medium is collisionless and no artificial viscosity is included in the simulation code (Smolsky & Usov 1996). Thermalization of the electron distribution is purely a result of collisionless interactions between particles and electromagnetic oscillations generated at the wind front.

At $\Gamma_e \leq 700\Gamma_0$, the fit of the electron spectrum by a two-dimensional relativistic Maxwellian (21) with $\Gamma_T \simeq 200\Gamma_0$ is rather accurate (see Fig. 9). A small excess of electrons with Lorentz factors $\Gamma_e > 700\Gamma_0$ may be interpreted as a high-energy tail. Such a tail may result, for example, from multiple acceleration of high-energy electrons at the wind front. Figure 10 shows the angular distribution of high-energy electrons in the region far ahead of the wind front. From Figure 10, we can see that this distribution is anisotropic. The mean angle between the velocity of outflowing electrons and the normal to the wind front is $\langle\psi\rangle \simeq 1/3$ radian.

4.5. Synchro-Compton radiation of high-energy electrons from the region ahead of the wind front

High-energy electrons with a nearly Maxwellian spectrum are injected into the region ahead of the wind front and radiate in the fields of LAEMWs via synchro-Compton mechanism. The mean angle between the velocity of these electrons and the wave vector of LAEMWs is $\langle\psi\rangle \simeq 1/3$ radian. Using this and equations (7) and (20), we can see that the condition (15) is satisfied, and, therefore, in the region ahead of the wind front synchro-Compton radiation of high-energy electrons closely resembles synchrotron radiation. To model the spectrum of synchro-Compton radiation, we replace the fields of LAEMWs $B_z(t, x)$ and $E_y(t, x)$ by a constant magnetic field which is equal to the mean field of LAEMWs $\langle B_w \rangle$. The energy losses of electrons in such a magnetic field are governed by (Landau & Lifshitz 1971)

$$\frac{d\Gamma_e}{dt} = -\chi(\Gamma_e^2 - 1), \quad (22)$$

where $\chi = 2e^4 \langle B_w \rangle^2 / 3m_e^3 c^5$.

In our approximation, the evolution of the spectrum of high-energy electrons in the region ahead of the wind front may be found from the following equation (e.g., Pacholczyk 1969)

$$\frac{\partial f(\Gamma_e, t)}{\partial t} = \frac{\partial}{\partial \Gamma_e} [\chi \Gamma_e^2 f(\Gamma_e, t)] + \dot{N}_e f_{\text{bar}}(\Gamma_e), \quad (23)$$

where $f(\Gamma_e, t)$ is the distribution function of high-energy electrons in the region ahead of the wind front per unit area of the front at the moment t , $\dot{N}_e \simeq n_0 c$ is the rate of production of high-energy electrons per unit area of the front, and $f_{\text{bar}} = (\Gamma_e / \Gamma_T^2) \exp(-\Gamma_e / \Gamma_T)$ is the average spectrum of high-energy electrons which are injected into the region ahead of the front. The function $f(\Gamma_e, t)$ is normalized to the total number of high-energy electrons per unit area of the front N_e , while the function f_{bar} is normalized to unity:

$$\int_1^\infty f(\Gamma_e, t) d\Gamma_e = N_e \quad \text{and} \quad \int_1^\infty f_{\text{bar}} d\Gamma_e = 1. \quad (24)$$

For simplicity, we disregard the angular anisotropy of the electron distribution function.

Under the mentioned assumptions, in the frame of the wind front the differential proper intensity of synchro-Compton radiation from the region ahead of the wind front is (e.g., Pacholczyk 1969; Rybicki & Lightman 1979)

$$I_\nu(t) = \int_1^\infty f(\Gamma_e, t) i_\nu d\Gamma_e, \quad (25)$$

where

$$i_\nu = \frac{\sqrt{3} e^3 \langle B_w \rangle \nu}{m_e c^2} \frac{\nu}{\nu_c} \int_{\nu/\nu_c}^\infty K_{5/3}(\eta) d\eta, \quad (26)$$

is the spectrum of synchrotron radiation generated by a single relativistic electron in a uniform magnetic field $\langle B_w \rangle$, $K_{5/3}$ is the modified Bessel functions of 5/3 order and

$$\nu_c = \frac{3e \langle B_w \rangle \Gamma_e^2}{4\pi m_e c} \quad (27)$$

is the typical frequency of synchrotron radiation.

The observed spectral flux $F_\nu(t)$ (in units $\text{erg s}^{-1} \text{cm}^{-2} \text{erg}^{-1}$) can be obtained from the proper intensity $I_\nu(t)$ dividing by the square of the burster distance d , and by taking into account both the effects of relativistic beaming and cosmological effects (e.g., Tavani 1996a; Dermer 1998):

$$F_\nu(t) = \frac{D^3(1+z)}{4\pi d^2} I_{\nu'}(t), \quad (28)$$

where D is the relativistic Doppler factor, $D \simeq 2\Gamma_0$, and z is the cosmological redshift. The observed frequency ν depends on the emitted frequency ν' in the wind frame as $\nu = [D/(1+z)]\nu' \simeq [2\Gamma_0/(1+z)]\nu'$.

Equations (22) – (28) were integrated numerically. For typical parameters of cosmological γ -ray bursters, $\Gamma_0 = 150$, $B_0 = 300 \text{ G}$, $\langle B_w \rangle = 0.1B_0$, $\Gamma_T = 200\Gamma_0 = 3 \times 10^4$ and $z = 1$, Figure 11 shows the observed spectrum of synchro-Compton radiation from the region ahead of the wind front. For this radiation the characteristic energy of photons is in the BATSE range (e.g., Band et al. 1993; Schaefer et al. 1994; Fishman & Meegan 1995; Preece et al. 1996; Schaefer et al. 1998). The spectrum of synchro-Compton radiation displays a continuous hard to soft evolution, in agreement with observational data on GRBs (Bhat et al. 1994).

5. Conclusions and discussion

In a relativistic strongly magnetized wind outflowing from a fast rotating compact object like a millisecond pulsar with the surface magnetic field $B_s \sim 10^{15} - 10^{16} \text{ G}$, there are at least two regions where extremely powerful non-thermal emission in hard (X-ray and γ -ray) photons may be generated (see Fig. 1). The first radiating region is at the distance $r_f \sim 10^{13} - 10^{14} \text{ cm}$ from the compact object. In this region, the striped component of the wind field is transformed into LAEMWs. Acceleration of electrons in the fields of LAEMWs and generation of non-thermal radiation at $r \sim r_f$ were considered in (Usov 1994a,b; Blackman et al. 1996; Blackman & Yi 1998). The second radiating region is at $r \sim r_{\text{dec}} \sim 10^{16} - 10^{17} \text{ cm}$ where deceleration of the wind due to its interaction with an ambient medium becomes important. We have used one-and-a-half dimensional particle-in-cell plasma simulations to study both the interaction of a relativistic, strongly magnetized wind with an ambient medium at $r \sim r_{\text{dec}}$ and non-thermal radiation from the region of this interaction (Smolsky & Usov 1996; Usov & Smolsky 1998 and the present paper). One of the main results of this study is that we have confirmed the idea of Mészáros and Rees (1992) that the wind – ambient medium interaction may be

responsible for high-frequency (X-ray and γ -ray) emission of cosmological GRBs. We have shown that at $r \sim r_{\text{dec}}$, where in the wind frame the magnetic pressure of the wind is comparable to the dynamical pressure of the ambient medium, $\alpha \sim 1$, an essential part (about 20%) of the wind energy may be transferred to high-energy electrons and then to high-frequency emission. In this paper, it is shown that in the wind frame the spectrum of electrons which are accelerated at the wind front and move ahead of the front is close to a two-dimensional relativistic Maxwellian with the temperature $T = m_e c^2 \Gamma_T / k$, where Γ_T is equal to $200\Gamma_0$ with the accuracy of $\sim 20\%$. Our simulations point to the existence of a high-energy tail of accelerated electrons with a Lorentz factor of more than $\sim 700\Gamma_0$. It was shown in our early papers (Smolsky & Usov 1996; Usov & Smolsky 1998) that the process of the wind – ambient medium interaction is strongly nonstationary, and LAEMWs are generated by the oscillating currents at the wind front and propagate away from the front. In the wind frame, the mean field of LAEMWs in the region ahead of the wind front is $\langle B_w \rangle \simeq 0.1 B_{\text{dec}} / \Gamma_0 \sim 10 - 10^2$ G. High-energy electrons that are accelerated at the wind front and injected into the region ahead of the front generate synchro-Compton radiation in the fields of LAEMWs. This radiation closely resembles synchrotron radiation in a uniform magnetic field with the strength of $\langle B_w \rangle$. In the burster frame, for typical parameters of relativistic strongly magnetized winds outflowing from millisecond pulsars with extremely strong magnetic fields, $B_s \simeq 10^{15} - 10^{16}$ G, the maximum of synchro-Compton radiation generated in the region ahead of the wind front at $r \sim r_{\text{dec}}$ is in the BATSE range, from $\sim 10^2$ keV to a few MeV. Radiation which is generated at the wind front may be responsible for high-energy γ -rays, $\varepsilon_\gamma >$ a few ten MeV, which are observed in the spectra of some GRBs (Hurley et al. 1994). The energy flux of GRBs in such high-energy γ -rays may be more or less comparable with the energy flux in the BATSE range if $\Gamma_0 B_{\text{dec}} \gtrsim 3 \times 10^8$ G. Besides that, high-energy γ -rays may be generated efficiently via inverse Compton scattering (e.g., Jones & Hardee 1979; Mészáros, Rees & Papathanassiou 1994). In the burster frame, the spectrum of high-energy γ -rays generated at $r \sim r_{\text{dec}}$ may, in principle, extend up to the maximum energy of accelerated electrons which is about the maximum energy of protons reflected from the wind front, $\varepsilon_\gamma^{\text{max}} \sim m_p \Gamma_0^2 \sim 10^{13} (\Gamma_0 / 10^2)^2$ eV. In connection with this, it is worth noting that the Tibet air shower array (Amenomori et al. 1996) and HEGRA AIROBICC Cherenkov array (Padilla et al. 1998) have independently reported significant excesses of γ -rays at energies of $\sim 10^{13}$ eV coincident with some GRBs both in direction and burst time. The statistical significance of these results was estimated to be about 6σ . [For details on very high energy γ -rays from cosmological γ -ray bursters see (Totani 1998, 1999).]

To fit the observed spectra of GRBs, for accelerated electrons it was usually taken either a three-dimensional relativistic Maxwellian distribution (Katz 1994a,b) or a sum

of a three-dimensional relativistic Maxwellian distribution and a suprathermal power-law tail (Tavani 1996a,b). The thermal character of the electron distribution (or its part) is consistent with our results. In our simulations, we observe a two-dimensional relativistic Maxwellian distribution of accelerated electrons. However, the difference between 2D and 3D Maxwellian distributions does not change the calculated spectrum of synchrotron radiation significantly (Jackson 1975; Jones & Hardee 1979; Rybicki & Lightman 1979).

Our solution for the wind – ambient medium collision is completely self-consistent only if α is $\gtrsim \alpha_{\text{cr}} \simeq 0.4$ (Usov & Smolsky 1998). Such values of α are most interesting for cosmological GRBs because at $r \simeq r_{\text{dec}}$ when deceleration of a relativistic wind due to its interaction with the ambient medium becomes important the value of α is about unity. At $\alpha < \alpha_{\text{cr}}$, both the structure of the wind front and the process of the wind – ambient medium interaction are not studied well enough. For this case, we have constructed a solution with a strong surface current at the wind front (Smolsky & Usov 1996; Usov & Smolsky 1998). In this solution, the surface current is considered as an external one and fixed. Maybe, in the process of interaction of a relativistic strongly magnetized wind with an ambient medium at $\alpha < \alpha_{\text{cr}}$ the structure of the wind front is self-regulated so that a required current runs along the front.

A situation similar, in some respects, to our problem was considered in the works of Hoshino et. al (1992) and Gallant & Arons (1994), where collisionless shocks rather than the plasma beam – magnetic barrier collision were examined. In these studies, acceleration of light particles, electrons and positrons, was observed near the shock (Hoshino et al. 1992). The level of electron acceleration reported by Hoshino et. al (1992) is compatible with our results. Indeed, the energy that is transferred from protons to electrons depends on their mass ratio, m_p/m_e . For computational reasons, the mass ratio used by Hoshino et. al (1992) was small, $m_p/m_e = 20$. In our simulations, we use the realistic mass ratio, $m_p/m_e = 1836$. If we substitute $m_p/m_e = 20$ into equation (7), we obtain the mean Lorentz factor of accelerated electrons that coincides with the results of Hoshino et al. (1992) within uncertainties of their and our calculations. The energy spectrum of accelerated electrons in the simulations of Hoshino et. al (1992) is close to a relativistic Maxwellian too.

In our scenario, the rotational energy of compact objects (millisecond pulsars or post-merger objects) is a source of energy for emission of cosmological γ -ray bursters. This energy may be as high as a few $\times 10^{53}$ ergs. If radiation of the gravitational waves by the compact object is negligible, the rotational energy is transformed to the energy of a relativistic Poynting flux-dominated wind with the efficiency of $\sim 100\%$. In the case when the angle ϑ between the rotational and magnetic axes of the compact object is about $\pi/2$, almost all the energy of the wind is radiated in X-rays and γ -rays at $r \sim r_f$ (Usov 1994a;

Blackman et al. 1996; Blackman & Yi 1998). The maximum energy which may be radiated in hard photons at $r \sim r_{\text{dec}}$ is only a few times smaller than that at $r \sim r_f$. Hence, the total energy output in hard photons per GRB may be as high as $\sim 10^{53}$ ergs or even a few times more. This energy is sufficient for the explanation of the energetics of cosmological GRBs.

At $\vartheta \simeq \pi/2$, when the bulk of the wind energy is transferred into γ -rays at $r \sim r_f$, the residual energy of the wind at $r \gg r_f$ may be very small. In this case, afterglows which are generated at $r \gtrsim r_{\text{dec}}$ and accompany GRBs are weak irrespective of that the GRBs themselves may be quite strong. This may explain the fact that X-ray, optical and radio afterglows have been observed in some strong GRBs but not in others (e.g., Piran 1998 and references therein).

For interpretation of data on cosmological GRBs, the interaction of a relativistic wind with an ambient medium and non-thermal radiation generated at $r \sim r_{\text{dec}}$ were considered in many papers (see, for a review Piran 1998). All these considerations were usually carried out in the frame of the conventional model which was based on the following assumptions.

(1) Two collisionless shocks form: an external shock that propagates from the wind front into the ambient medium, and an internal shock that propagates from the wind front into the inner wind, with a contact discontinuity at the wind front between the shocked material.

(2) Electrons are accelerated at the shocks to very high energies.

(3) The shocked matter acquires embedded magnetic fields. The energy density of these fields is about the energy density of high-energy electrons accelerated by the shocks.

(4) Highly accelerated electrons generate high-frequency (X-ray and γ -ray) radiation of GRBs via synchrotron mechanism.

(5) The efficiency of conversion of the wind energy into accelerated electrons and then to high-frequency radiation of GRBs is about 10% \sim 30%.

The idea about formation of two collisionless shocks near the front of a relativistic wind outflowing from a cosmological γ -ray burster is based mainly on both theoretical studies which have shown that collisionless shocks can form in a rarified plasma (e.g., Sagdeev 1962, 1979; Tidman & Krall 1971, Dawson 1983; Quest 1985) and the fact that such shocks have been observed in the vicinities of a few comets and planets (Leroy et al. 1982; Livesey, Kennel, & Russell 1982; Omid & Winske 1990 and references therein). Undoubtedly, collisionless shocks exist and can accelerate electrons to ultrarelativistic energies in many astrophysical objects such as supernova remnants and jets of active galactic nuclei. However, for the wind parameters which are relevant to cosmological GRBs (see § 2), formation of

collisionless shocks in the vicinity of the wind front is very questionable (e.g., Smolsky & Usov 1996; Mitra 1996; Brainerd 1999). Indeed, the properties of relativistic, transverse, magnetosonic collisionless shocks were studied in details by Gallant et al. (1992) and Hoshino et al. (1992), and it was shown that all the upstream ions are electromagnetically reflected from the shock front. This is similar to reflection of ions from the wind front in our simulations. If a shock forms, its thickness is of the order of the gyroradius of reflected protons in the upstream magnetic field (e.g., Hoshino et al. 1992). In a plasma system, a collisionless shock may form only if the characteristic size of the system is significantly larger than the shock thickness. In our case, the radius, r , of the wind front is the characteristic size of the system. At $r \sim r_{\text{dec}}$, an external collisionless shock may form in an ambient medium just ahead of the wind front if the the gyroradius of protons which are reflected from the wind front is significantly smaller than r_{dec} . In the burster frame, the gyroradius of reflected protons in the ambient medium is

$$R_{Bp} = \frac{m_p c^2 \Gamma_p}{e B_{\text{am}}} \simeq 3 \times 10^{16} \left(\frac{\Gamma_0}{10^2} \right)^2 \left(\frac{B_{\text{am}}}{10^{-6} \text{ G}} \right)^{-1} \text{ cm}, \quad (29)$$

where $\Gamma_p \simeq \Gamma_0^2$ is the mean Lorentz factor of reflected protons and B_{am} is the mean magnetic field of the ambient medium. For the interstellar medium in our Galaxy, the mean magnetic field is about 2×10^{-6} G (e.g., Manchester & Taylor 1977). If for a GRB the value of B_{am} is $\sim 2 \times 10^{-6}$ G, from equations (4) and (29), for the wind parameters which are relevant to cosmological GRBs (see § 2) we have $R_{Bp}/r_{\text{dec}} \sim 1$ at $\Gamma_0 = 10^2$ and $R_{Bp}/r_{\text{dec}} \sim 10^2$ at $\Gamma_0 = 10^3$. In this case, an external collisionless shock cannot form ahead of the wind front, especially if Γ_0 is about 10^3 or even more. Recently, Brainerd (1999) came to the same conclusion from another consideration. As to the internal shock, it cannot form in a Poynting flux-dominated wind too (e.g., Kennel, Fujimura & Okamoto 1983; Kennel & Coroniti 1984).

Our model of the wind – ambient medium interaction differs qualitatively from the conventional model which is based on the assumption that an external collisionless shock forms just ahead of the wind front. Although it might seem that observational consequences of our model must differ from observational consequences of the conventional model significantly, this is not the case. Moreover, we can see that all the listed assumptions of the conventional model are confirmed by our simulations, certainly except of the first assumption on formation of the collisionless shocks. There is only a modification that LAEMWs are embedded in the region ahead of the wind front instead of magnetic fields, and highly accelerated electrons generate high-frequency emission of GRBs via synchro-Compton radiation. However, in our case synchro-Compton radiation closely resembles synchrotron radiation. Therefore, if in the conventional model of GRB emission

from the shocked region ahead of the wind front the mechanism of electron acceleration by a relativistic, collisionless shock is replaced by the mechanism of electron acceleration at the wind front, this model will remain otherwise practically unchanged.

At $r > r_{\text{dec}}$, the outflowing wind slows down due to its interaction with the ambient medium, and when the Lorentz factor of the wind front is about several tens or less, an external shock may form just ahead of the front. We believe that the afterglows which are observed in $\sim 10^5$ s after some GRBs result from acceleration of electrons by such a shock as it is generally accepted (Mészáros & Rees 1997b; Vietri 1997; Waxman 1997; Wijers, Rees, & Mészáros 1997).

This research was supported by MINERVA Foundation, Munich / Germany.

REFERENCES

- Amenomori, M., et al. 1996, *A&A*, 311, 919
- Band, D., et al. 1993, *ApJ*, 413, 281
- Baring, M.G., & Harding, A.K. 1997, *ApJ*, 491, 663
- Benford, G. 1984, *ApJ*, 282, 154
- Bhat, P.N. et al. 1994, *ApJ*, 426, 604
- Blackman, E.G. & Yi, I. 1998, *ApJ*, 498, L31
- Blackman, E.G., Yi, I., & Field, G.B. 1996, *ApJ*, 473, L79
- Blandford, R.D., & Eichler, D. 1987, *Phys. Rep.*, 154, 1
- Blaes, O.M. 1994, *ApJS*, 92, 643
- Blumenthal, G.R. & Tucker, W.H. 1974, in *X-Ray Astronomy*, ed. R. Giacconi and H. Gursky (Dordrecht : D. Reidel Publishing Company), p. 99
- Brainerd, J.J. 1999, *astro-ph/9904040*
- Coroniti, F.V. 1990, *ApJ*, 349, 538
- Dai, Z.G., & Lu, T. 1998, *A&A*, 333, L87
- Dawson, J.M. 1983, *Rev. Mod. Phys.*, 55, 403
- Dermer, C.D. 1998, *ApJ*, 501, L157
- Dermer, C.D., & Weiler, T.J. 1995, *Ap&SS*, 231, 377
- Eichler, D., Livio, M., Piran, T. & Schramm, D. 1989, *Nature*, 340, 126
- Fenimore, E.E., Epstein, R.I., & Ho, C. 1993, *A&AS*, 97, 59
- Fishman, G.J. & Meegan, C.A. 1995, *ARA&A*, 33, 415
- Gaensler, B.M., Brazier, K.T.S., Manchester, R.N., & Johnston, S. 1999, *astro-ph/9901262*
- Gallant, Y.A., & Arons, J. 1994, *ApJ*, 435, 230
- Gallant, Y.A., Hoshino, M., Langdon, A.B., Arons, J., & Max, C.E. 1992, *ApJ*, 391, 73

- Goodman, J. 1986, ApJ, 308, L47
- Goodman, J., Dar, A., & Nussinov, S. 1987, ApJ, 314, L7
- Greiner, J. 1998, astro-ph/9802222
- Gunn, J.E. & Ostriker, J.P. 1971, ApJ, 165, 223
- Harding, A.K. 1994, ApJS, 90, 863
- Hartmann, D. 1995, in The Gamma-Ray Sky with *Compton GRO* and SIGMA, NATO ASI Proc. 461, ed. M. Signore, P. Salati, & G. Vedrenne (Dordrecht : Kluwer), 329
- Herster, J.J. 1998, in Neutron Stars and Pulsars: Thirty Years after the Discovery, ed. N. Shibazaki, N. Kawai, S. Shibata, & T. Kifune (Tokyo : Universal Academy Press), 431
- Hoshino, M., Arons J., Gallant, Y.A., & Langdon, A.B. 1992, ApJ, 390, 454
- Hurley, K., et al. 1994, Nature, 372, 652
- Jackson, J.D. 1975, Classical Electrodynamics (New York : Wiley)
- Janka, H.-Th., & Ruffert, M. 1996, A&A, 1996, 307, L33
- Jones, T.W., & Hardee, P.E. 1979, ApJ, 228, 268
- Katz, J. 1994a, ApJ, 432, L107
- Katz, J. 1994b, in Gamma-Ray Bursts, Second Workshop, ed. G.J. Fishman, J.J. Brainerd, & K. Hurley (New York: AIP), 529
- Katz, J. 1997, ApJ, 490, 633
- Kennel, C.F., & Coroniti F.V. 1984, ApJ, 283, 694
- Kennel, C.F., Fujimura, F.S., & Okamoto, I. 1983, J. Ap. Geophys. Fluid Dyn., 26, 147
- Kluźniak, W., & Ruderman, M. 1998, ApJ, 505, L113
- Kulkarni, S.R., et al. 1998, Nature, 393, 35
- Kulkarni, S.R., et al. 1999, Nature, 398, 389
- Landau, L.D., & Lifshitz, E.M. 1971, The Classical Theory of Fields (Elmsford : Pergamon Press)

- Leroy, M.M., Winske, D., Goodrich, C.C., Wu, C.S., & Papadopoulos, K. 1982, *J. Geophys. Res.*, 87, 5081
- Lipunov, V.M., Postnov, K.A., Prokhorov, M.E., Panchenko, I.E., & Jorgensen, H.E. 1995, *ApJ*, 454, 593
- Livesey, W.A., Kennel, C.F., & Russell, C.T. 1982, *Geophys. Res. Lett.*, 9, 1037
- Manchester, R.N. & Taylor, J.H. 1977, *Pulsars* (San Francisco : Freeman)
- Meegan, C.A., Fishman, G.J., Wilson, R.B., Paciesas, W.S., Pendleton, G.N., Horack, J.M., Brock, M.N., & Kouveliotou, C. 1992, *Nature*, 355, 143
- Meegan, C.A., et al. 1994, in *Gamma-Ray Bursts, Second Workshop*, ed. G.J. Fishman, J.J. Brainerd, & K. Hurley (New York: AIP), 3
- Melatos, A. & Melrose, D.B. 1996a, *MNRAS*, 279, 1168
- Melatos, A. & Melrose, D.B. 1996b, *ASP Conf. Ser.*, 105, 421
- Mészáros, P., & Rees, M.J. 1992, *ApJ*, 397, 570
- Mészáros, P., & Rees, M.J. 1993, *ApJ*, 405, 278
- Mészáros, P., Rees, M.J., & Papathanassiou, H. 1994, *ApJ*, 432, 181
- Mészáros, P., & Rees, M.J. 1997, *ApJ*, 482, L29
- Mészáros, P., & Rees, M.J. 1997, *ApJ*, 476, 232
- Metzger, R.M. et al. 1997, *Nature*, 387, 879
- Michel, F.C. 1971, *Comments Ap. Space Phys.*, 3, 80
- Michel, F.C. 1985, *ApJ*, 288, 138
- Mitra, A. 1996, *A&A*, 313, L9
- Narayan, R., Paczyński, B., & Piran, T. 1992, *ApJ*, 395, L83
- Omidi, N., & Winske, D. 1990, *J. Geophys. Res.*, 95, 2281
- Pacholczyk, A.G. 1969, *Radio Astrophysics* (San Francisco : Freeman)
- Paczyński, B. 1986, *ApJ*, 308, L43

- Paczyński, B. 1991, *Acta Astron.*, 41, 257
- Padilla, L., et al. 1998, *A&A*, 337, 43
- Perna, R., & Loeb, A. 1998, *ApJ*, 509, L85
- Piran, T. 1998, astro-ph/9810256
- Preece, R.D., et al. 1996, *ApJ*, 473, 310
- Quest, K.B. 1985, *Phys. Rev. Lett.*, 54, 1872
- Rees, M.J., & Mészáros, P. 1992, *MNRAS*, 258, 41
- Rybicki, G.B., & Lightman, A.P. 1979, *Radiative Processes in Astrophysics* (New York : John Wiley & Sons)
- Sagdeev, R.Z. 1962, *Sov. Phys. Tech. Phys.*, 6, 867
- Sagdeev, R.Z. 1979, *Rev. Mod. Phys.*, 51, 11
- Schaefer, B.E., et al. 1994, *ApJS*, 92, 285
- Schaefer, B.E., et al. 1998, *ApJ*, 492, 696
- Smolsky, M.V., & Usov, V.V. 1996, *ApJ*, 461, 858
- Sulkanen, M.E., & Lovelace, R.V.E. 1990, *ApJ*, 350, 732
- Tamblyn, P., & Melia, F. 1993, *ApJ*, 417, 421
- Tavani, M. 1996a, *ApJ*, 466, 768
- Tavani, M. 1996b, *Phys. Rev. Lett.*, 76, 3478
- Thompson, C., & Duncan, R.C. 1993, *ApJ*, 408, 194
- Tidman, D.A., & Krall, N.A. 1971, *Shock waves in collisionless plasma* (New York : Wiley)
- Totani, T. 1998, *ApJ*, 509, L81
- Totani, T. 1999, *Astropart. Phys.*, in press (astro-ph/9810207)
- Usov, V.V. 1975, *Ap&SS*, 32, 375
- Usov, V.V. 1992, *Nature*, 357, 472

- Usov, V.V. 1994a, MNRAS, 267, 1035
- Usov, V.V. 1994b, in Gamma-Ray Bursts, Second Workshop, ed. G.J. Fishman, J.J. Brainerd, & K. Hurley (New York: AIP), 552
- Usov, V.V., & Chibisov, G.V. 1975, Soviet Astron., 19, 115
- Usov, V.V., & Smolsky, M.V. 1998, Phys. Rev. E, 57, 2267
- van den Berg, S. 1983, Ap&SS, 97, 385
- Vietri, M. 1996, ApJ, 471, L95
- Vietri, M. 1997, ApJ, 478, L9
- Waxman, E. 1997, ApJ, 485, L5
- Wijers, R.A.M.J., Rees, M.J., & Mészáros, P. 1997, MNRAS, 288, 51P
- Wickramasinghe, W.A.D.T., Nemiroff, R.J., Norris, J.P., Kouveliotou, C., Fishman, G.J., Meegan, C.A., Wilson, R.B., & Paciesas, W.S. 1993, ApJ, 411, L55
- Woosley, S.E. 1993, A&A, 97, 205
- Yi, I., & Blackman, E.G. 1998, ApJ, 494, L163

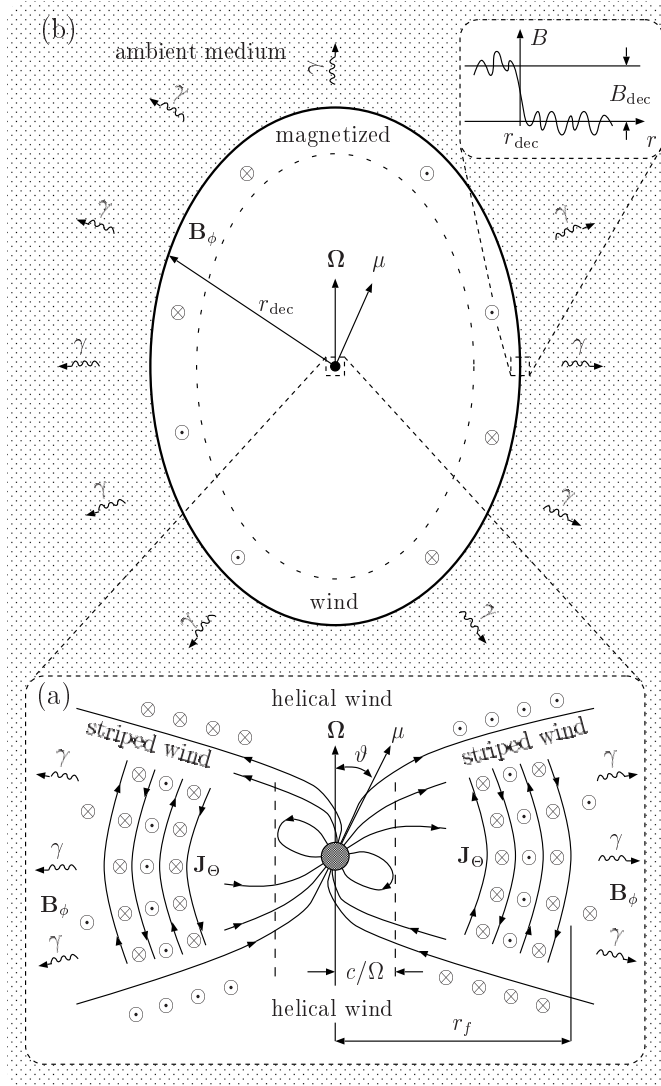


Fig. 1.— Sketch (not to scale) of the region where a GRB is generated by a relativistic strongly magnetized wind. This wind is produced by a fast-rotating compact object like a millisecond pulsar with the angular velocity Ω and the magnetic moment μ , $|\Omega| \sim 10^4 \text{ s}^{-1}$ and $|\mu| \simeq B_s R^3 \sim 10^{34} \text{ G cm}^3$. The figure part (a) shows a plausible magnetic topology of the outflowing wind at the moment when the front of the wind is at the distance $r \sim r_f$ from the compact object. At this distance, the striped component of the wind field is transformed into LAEMWs which decay fast, and γ -rays are generated. At $r \gg r_f$, the magnetic field is helical everywhere in the wind. The figure part (b) shows the region of the wind – ambient medium interaction when r is $\sim r_{\text{dec}}$. The main part of the wind energy is concentrated between the wind front (thick solid elliptic line) and the dotted elliptic line. In the right upper corner of (b), it is shown the distribution of magnetic fields in the enlarged vicinity of the front. These fields are a superposition of the wind field which is $B_{\text{dec}}\Theta(r_{\text{dec}} - r)$ and the fields of LAEMWs generated at the wind front. In the region ahead of the wind front, electrons of the ambient medium which are accelerated at the front to extremely high energies move in the fields of LAEMWs and generate synchro-Compton γ -rays. Directions of γ -ray propagation are shown by arrows with wavy lines.

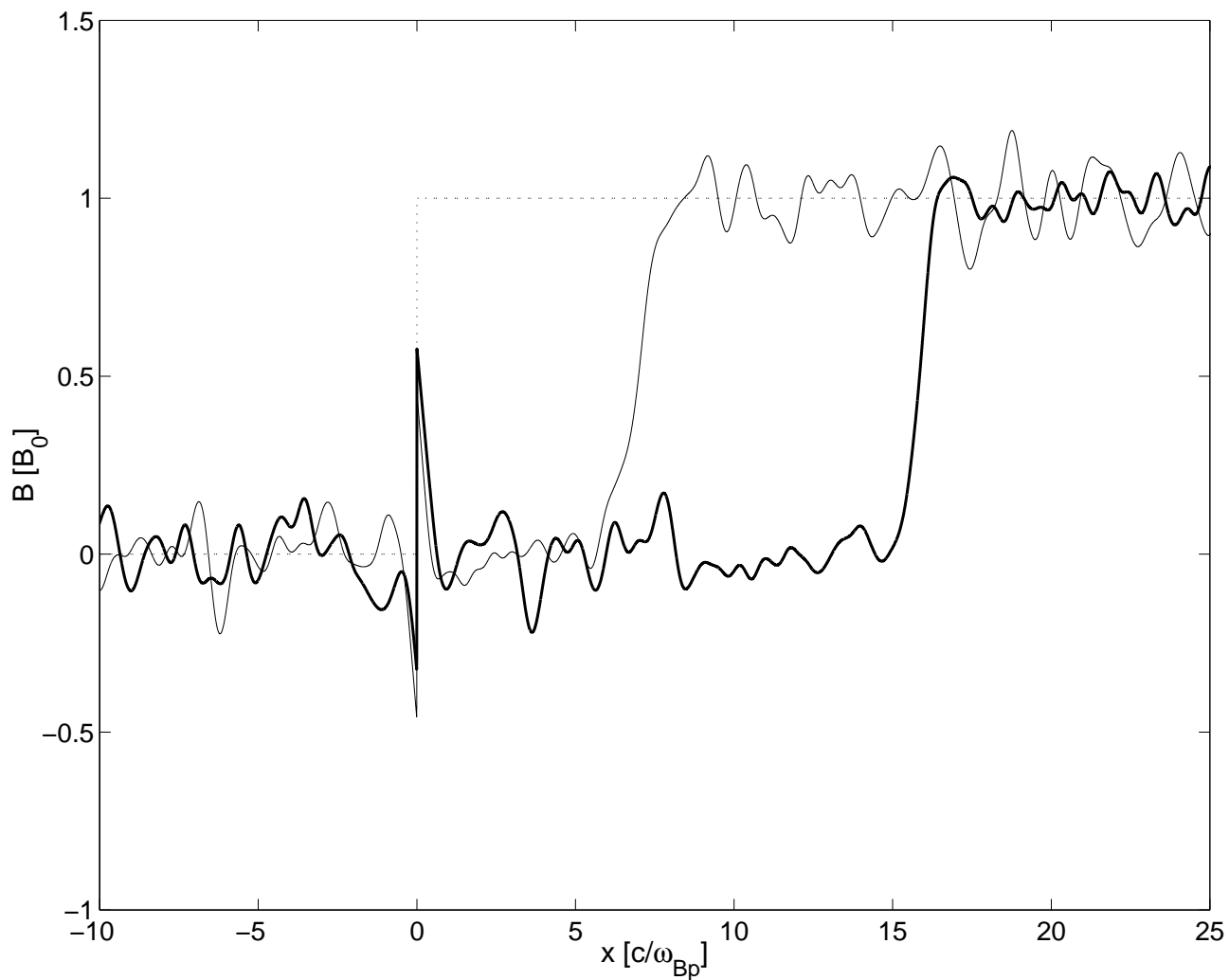


Fig. 2.— Distribution of magnetic field for a simulation with $B_0 = 300$ G, $\Gamma_0 = 300$ and $\alpha = 2/3$ at the moments $t = 0$ (dotted line), $t = 7.96T_p$ (thin solid line), and $t = 15.9T_p$ (thick solid line). $T_p = 2\pi m_p c \Gamma_0 / e B_0$ is the proton gyroperiod in the magnetic field, B_0 , of the barrier.

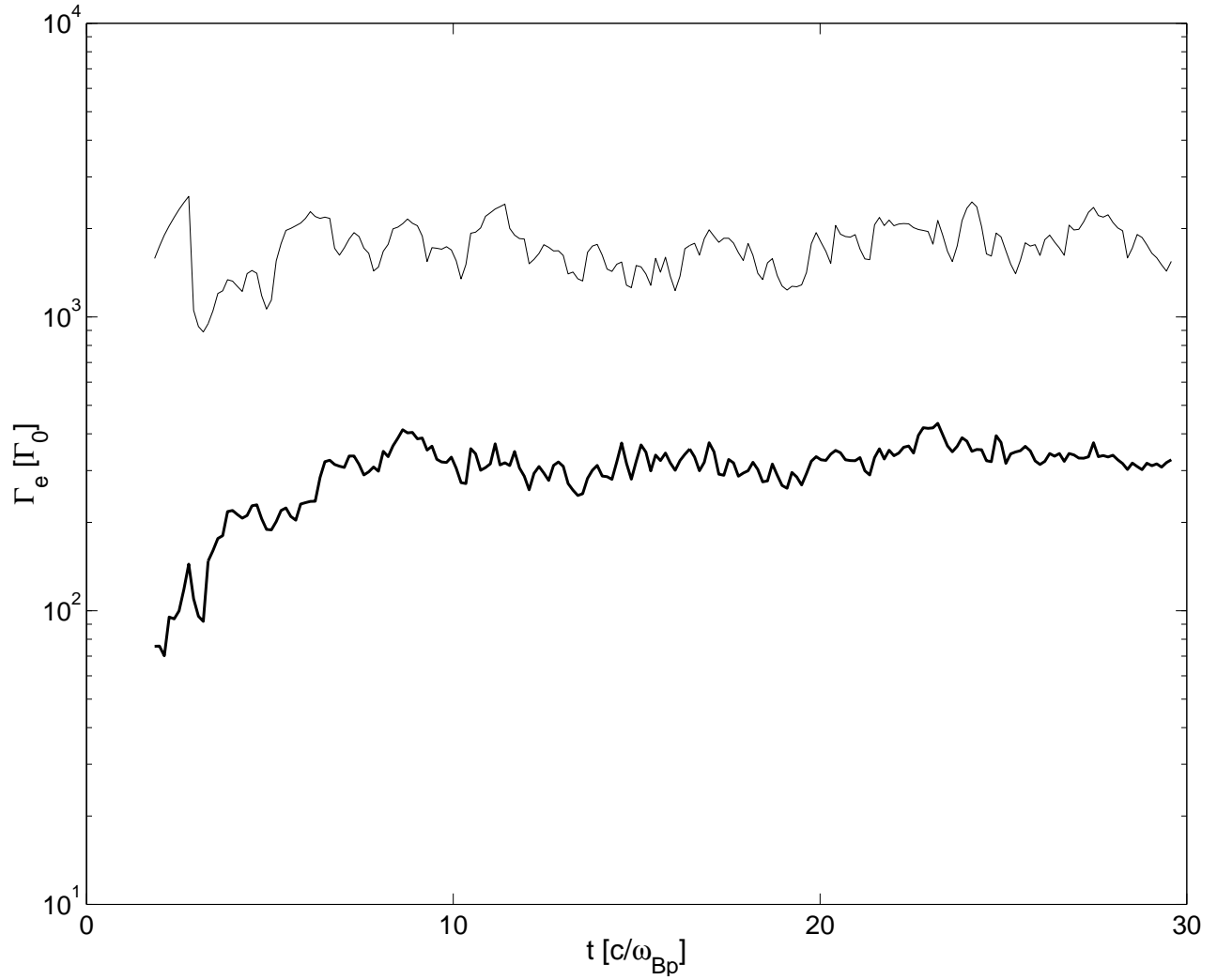


Fig. 3.— Maximum (thin line) and mean (thick line) energies of outflowing electrons, $v_x < 0$, at $x < 0$ after their reflection from the barrier in a simulation with $B_0 = 300$ G, $\Gamma_0 = 300$ and $\alpha = 2/3$.

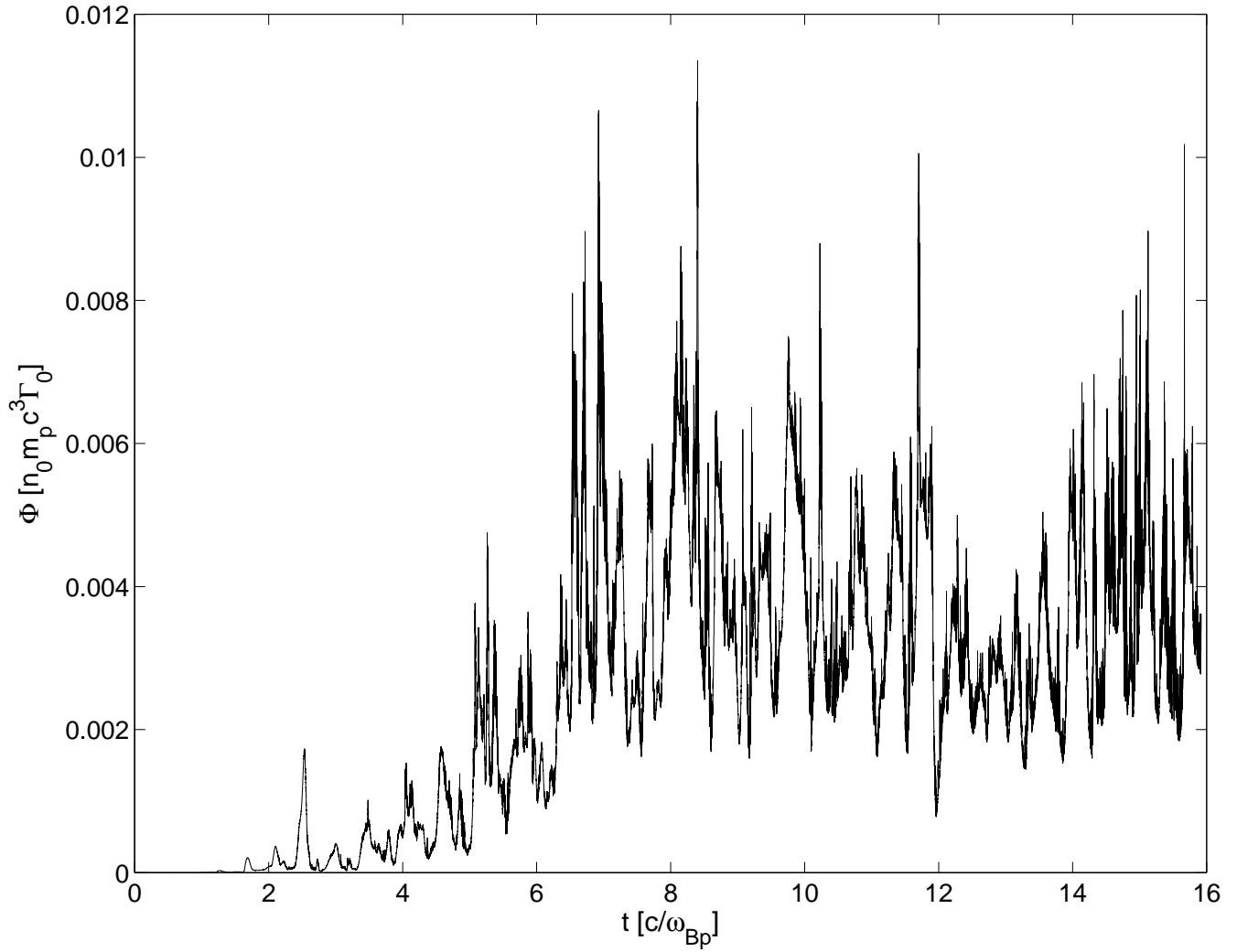


Fig. 4.— Intensity of synchrotron radiation of highly accelerated electrons per unitary area of the front of the magnetic barrier in a simulation with $B_0 = 300$ G, $\Gamma_0 = 300$ and $\alpha = 2/3$.

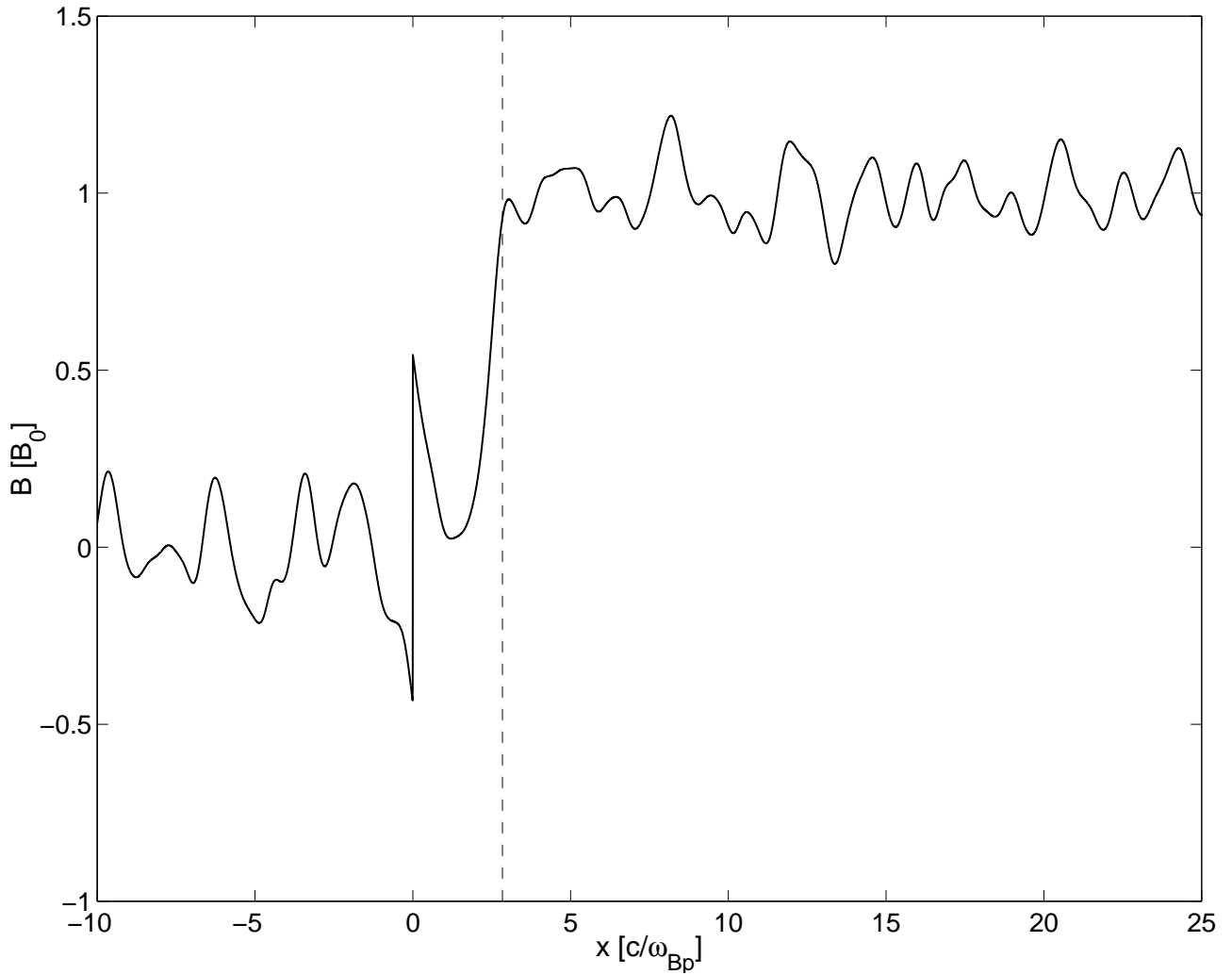


Fig. 5.— Distribution of magnetic field for a simulation with $B_0 = 300$ G, $\Gamma_0 = 300$ and $\alpha = 1/2$ at the moment $t = 15.92T_p$. The depth of the beam particle penetration into the barrier, $x_{\text{pen}} = 2.84(c/\omega_{Bp})$, is shown by dashed line.

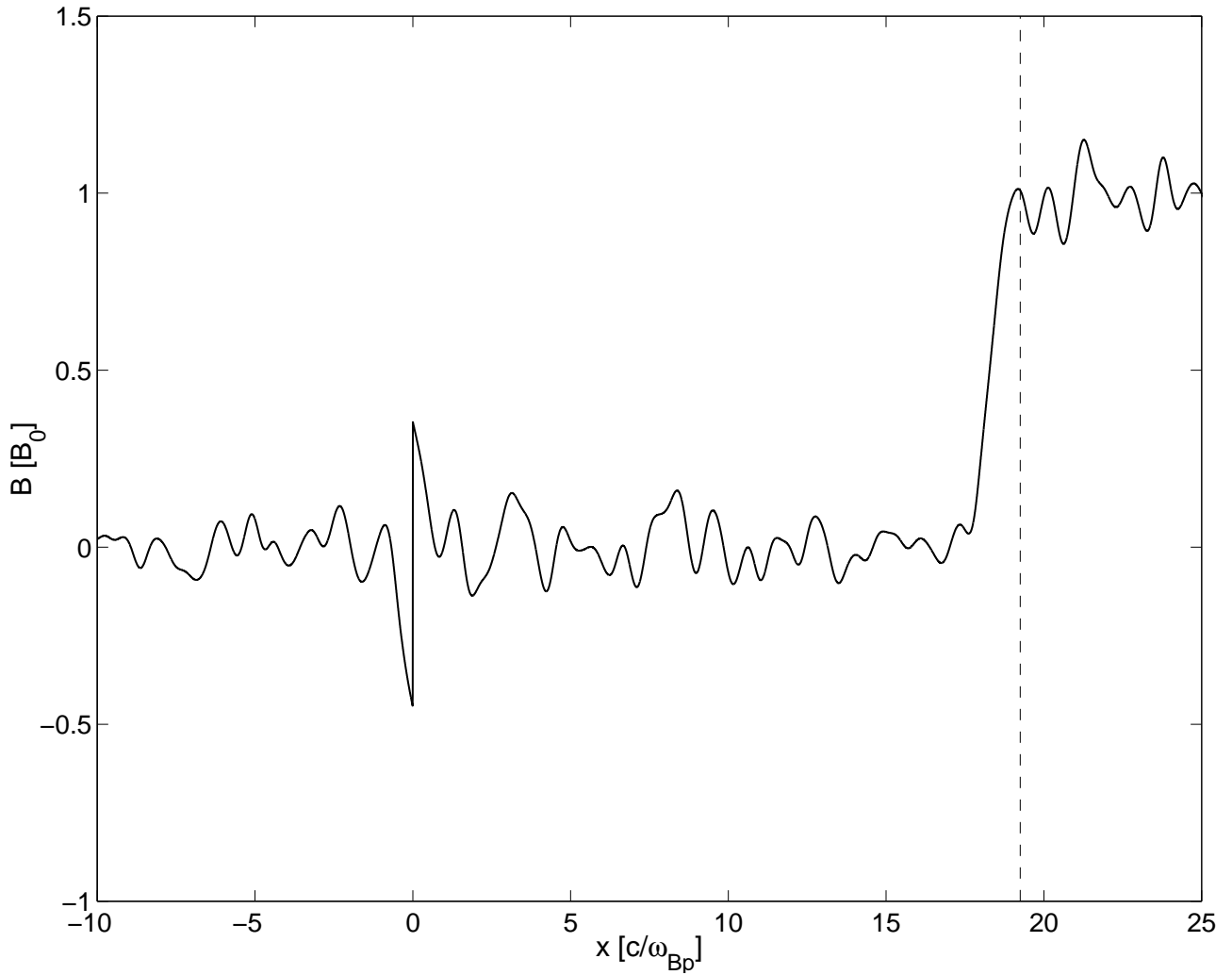


Fig. 6.— Distribution of magnetic field for a simulation with $B_0 = 300$ G, $\Gamma_0 = 300$ and $\alpha = 1$ at the moment $t = 15.92T_p$. The depth of the beam particle penetration into the barrier, $x_{\text{pen}} = 19.25(c/\omega_{Bp})$, is shown by dashed line.

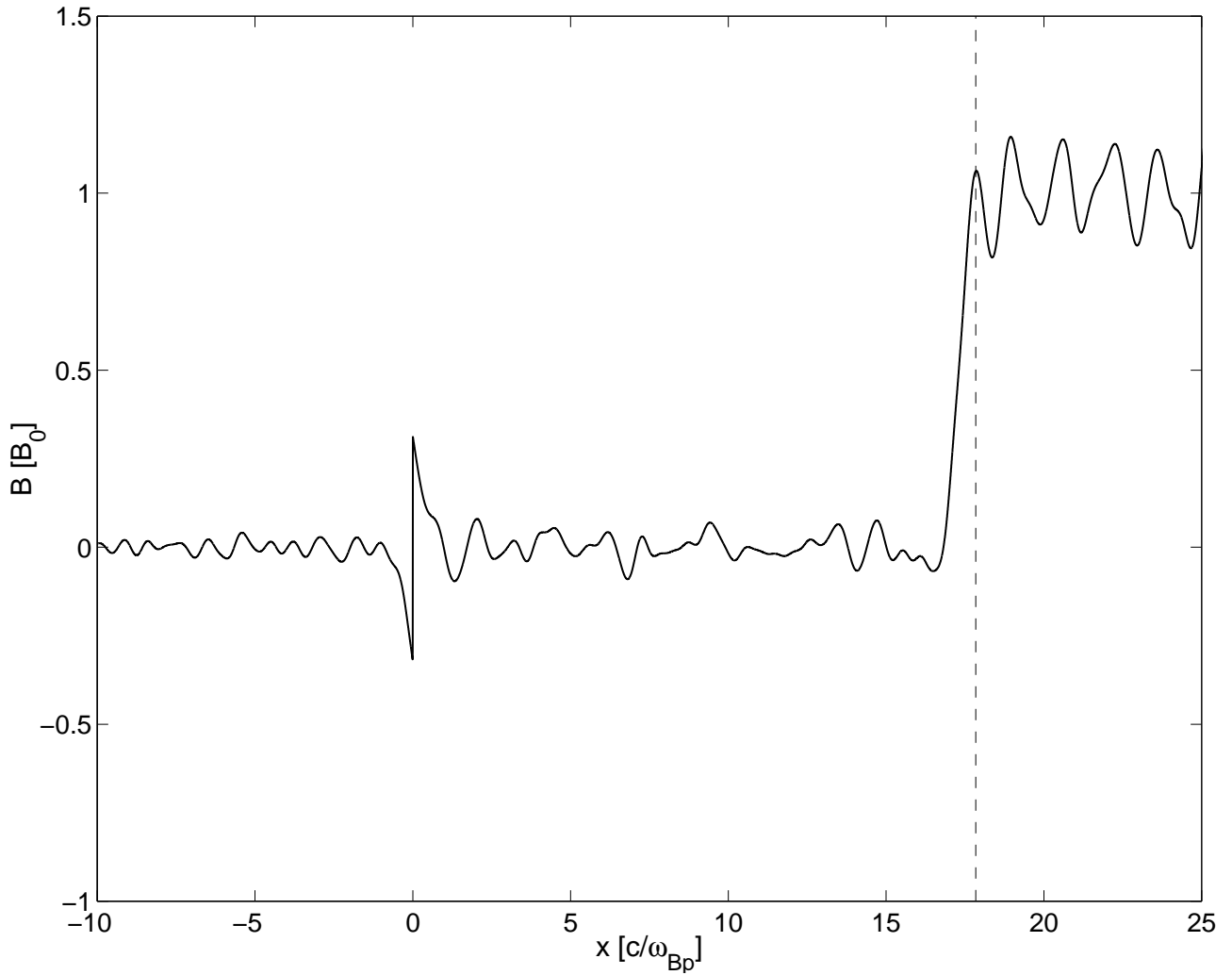


Fig. 7.— Distribution of magnetic field for a simulation with $B_0 = 300$ G, $\Gamma_0 = 300$ and $\alpha = 2$ at the moment $t = 7.96T_p$. The depth of the beam particle penetration into the barrier, $x_{\text{pen}} = 17.84(c/\omega_{Bp})$, is shown by dashed line.

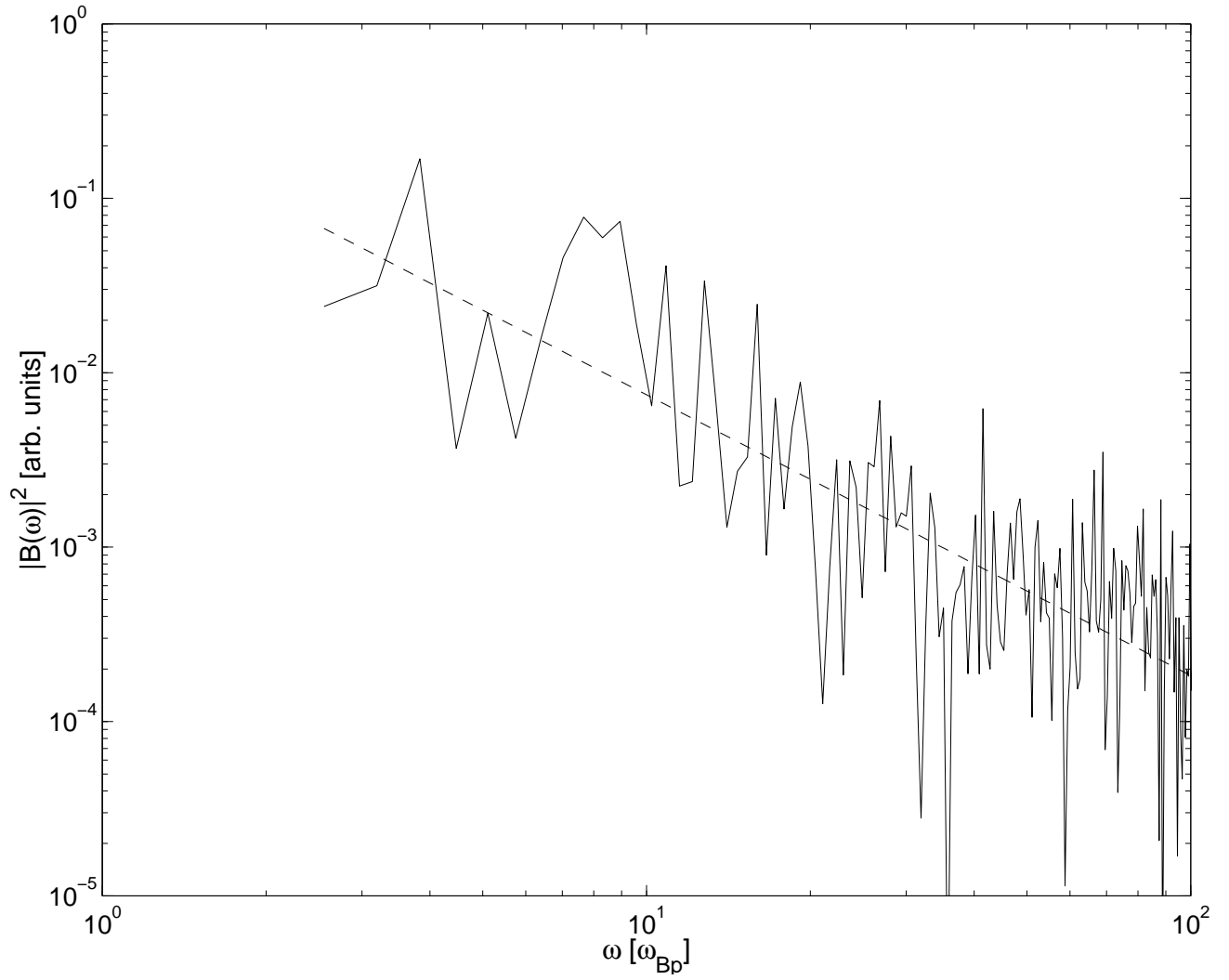


Fig. 8.— Power spectrum of low-frequency electromagnetic waves generated at the front of the barrier in a simulation with $B_0 = 300$ G, $\Gamma_0 = 300$ and $\alpha = 2/3$. The spectrum is fitted by a power law (dashed line).

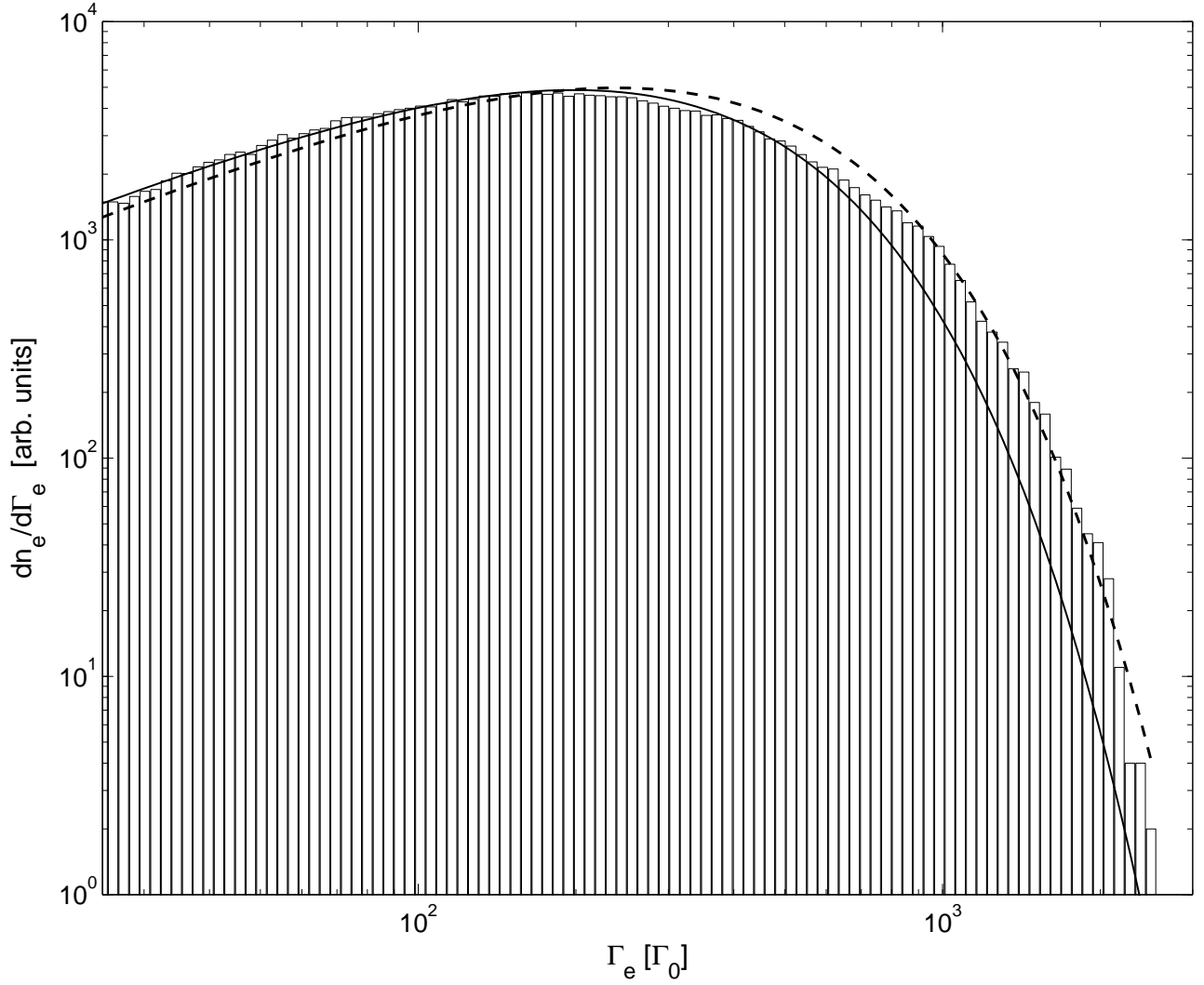


Fig. 9.— Energy spectrum of highly accelerated electrons in the region ahead of the wind front in the frame of the wind for a simulation with $B_0 = 300$ G, $\Gamma_0 = 300$ and $\alpha = 2/3$. The electron spectrum is fitted by a two-dimensional relativistic Maxwellian with a relativistic temperature $T = m_e c^2 \Gamma_T / k$, where Γ_T is equal to either $240\Gamma_0$ (dashed line) or $200\Gamma_0$ (solid line).

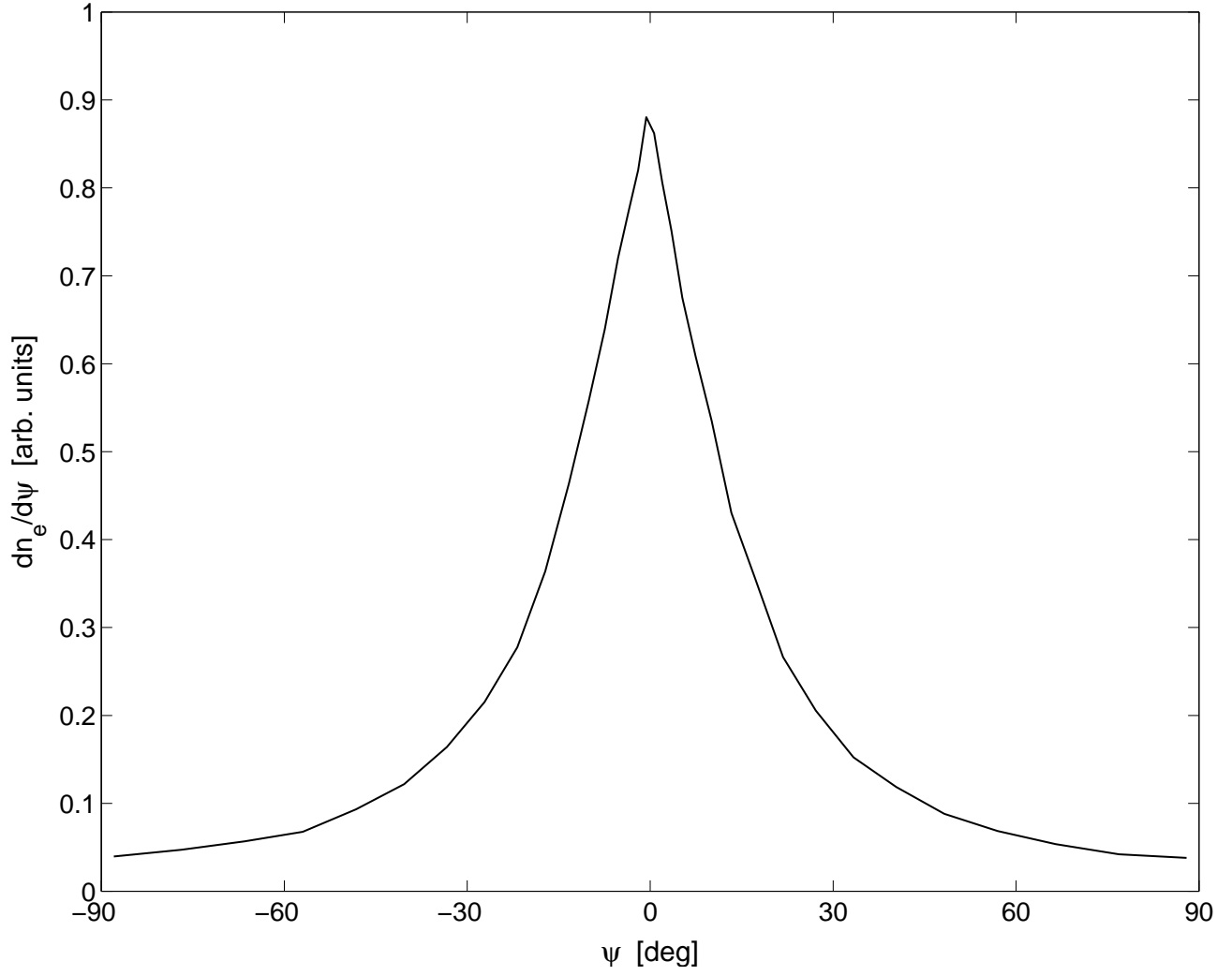


Fig. 10.— Angular distribution of outflowing high-energy electrons in a simulation with $B_0 = 300$ G, $\Gamma_0 = 300$ and $\alpha = 2/3$.

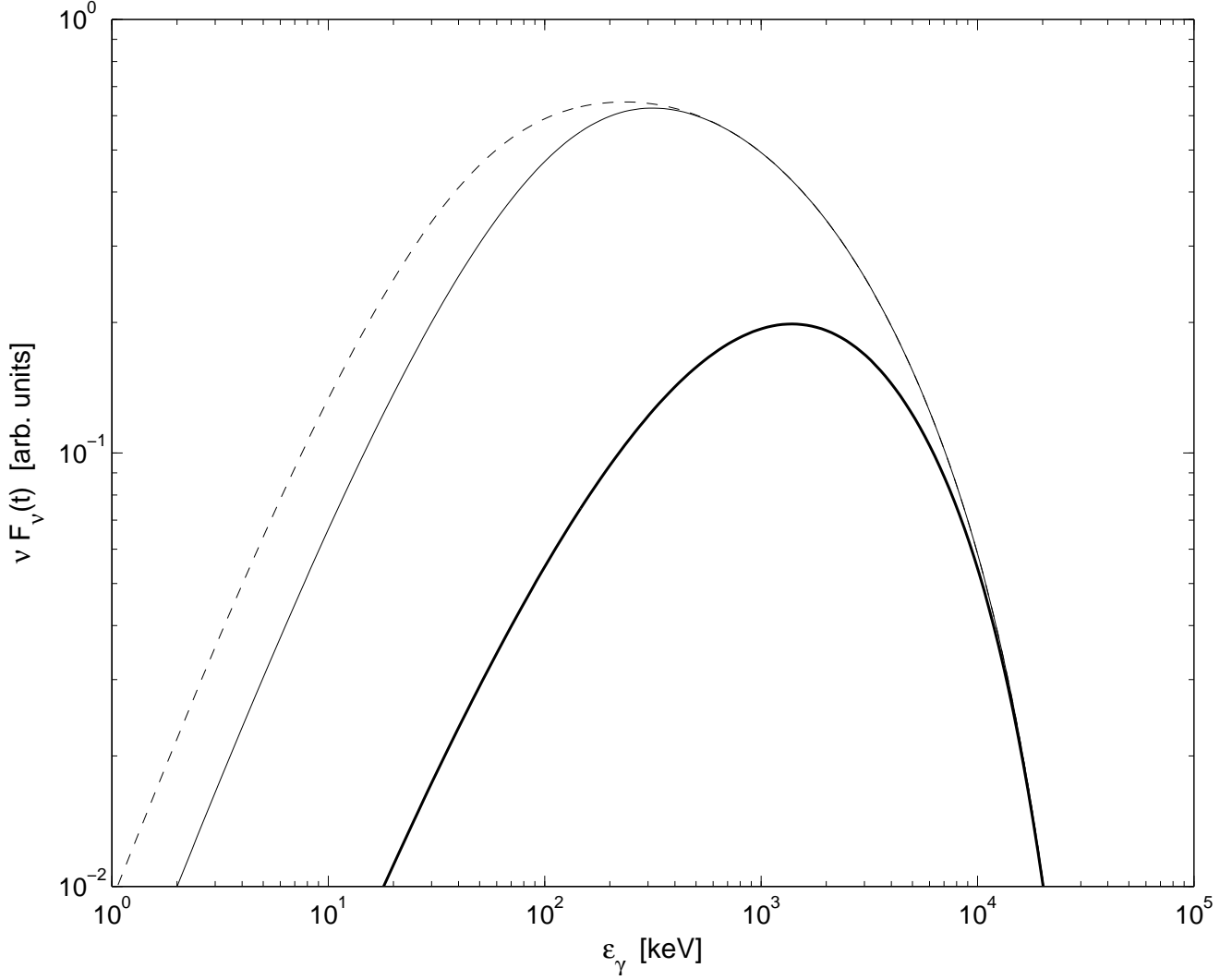


Fig. 11.— Calculated spectral power of synchro-Compton radiation from the region ahead of the wind front as a function of photon energy for $\Gamma_0 = 150$, $B_0 = 300$ G, $\langle B_w \rangle = 0.1B_0$, $\Gamma_T = 200\Gamma_0 = 3 \times 10^4$ and $z = 1$. The spectrum of radiation is given for the moments when the fraction of the energy of high-energy electrons injected into the region ahead of the wind front which is radiated is nearly zero (thick solid line), 36% (thin solid line) and 58% (dashed line).